A UBV Study of the Fields Surrounding Two Long-Period Cepheids and an Adjacent Open Cluster in Carina

© T. A. Danks   July 1987

A thesis submitted in partial fulfillment of the
requirements for the degree of Master
of Science (Astronomy)

Saint Mary's University

Halifax, Nova Scotia

Table of Contents

Signatures of the Examining Committee

Dr. G.F. Mitchell
Professor and Chairman
Department of Astronomy

Dr. D.G. Turner (Thesis Supervisor)
Associate Professor of Astronomy

Dr. G.A. Welch.
Associate Professor of Astronomy

Dr. B.C. Reed
Assistant Professor of Physics

Acknowledgements

I express gratitude to my advisor Dr. D.G. Turner. He suggested this project, supervised the work at every stage and critically reviewed three preliminary drafts. Credit for any originality or scientific value contained herein, however diminutive and fleeting, must be his rather than my own. Any conceptual flaws or errors of omission which remain are, of course, the responsibility of none other than myself.

I also thank Mr. W.G. Lumsden, the Officer-In-Charge of the Canadian Forces Meteorological and Oceanographic Centre (METOC). As my superior in the Canadian Forces Weather Service he tolerated my keeping flexible hours over the past six years while engaged in study at Saint Mary's. He also permitted liberal usage of the centre's not inconsiderable computing facilities without which data reduction and diagram preparation would have been a more onerous task.

My wife, Martha, endured much over the years of study culminating with this work. Untended chores, unpredictable hours and periods of preoccupation on my part made her life more difficult than it should have been. The few Saturday evenings not already lost to the demands of shift work seemed too frequently to be

disrupted by public tours at the Burke-Gaffney Observatory. She is understandably relieved to see this work concluded.

Finally I acknowledge the encouragement of Dr. J.N. Scrimger and the hospitality of his wife Judy. Were it not for the enthusiam generated in his 'Stars and Stellar Systems' course I would not have embarked on this sometimes unexpectedly long but ultimately rewarding road.

Abstract

A UBV Study of the Fields Surrounding

Two Long-Period Cepheids and an Adjacent

Open Cluster in Carina

T.A. Danks   July 1987

In continuation of a search for long-period [P>10d]
Cepheids embedded in associations (van den Bergh et al.
1982, 1983, 1984) U, B and V plates centered on the 13.2d
Cepheid GT Carinae, and including the Cepheid U Carinae and
the open cluster Trumpler 17, were measured on a Cuffey
Iris Astrophotometer. Colour-magnitude (CM) and colour-
colour (CC) diagrams for measured stars were examined on
the basis that any association of young stars to which GT
Car belongs would be apparent as a well defined main-sequence
in the CM plane and as a distinct group of OB stars sharing
common reddenings in the CC diagram. A variable extinction
analysis of the GT Car field indicates that the Cepheid is
more distant than the detected OB stars associated with
the Carina OB1 nebula complex. Detection of any OB stars
at the distance of GT Car would require a search to a
much fainter limiting magnitude than could be reached
in this study.

The field of the open cluster Trumpler 17 was also measured and analysed in a similar fashion using the same plates. Its distance of 2.0 ± 0.4 kpc places it in the foreground with respect to the Car OB1 complex and its age of $50(\pm 11)\times 10^6$ years makes it older than the OB stars belonging to this association.

An analysis of the reddenings, distance moduli and radial velocities for southern OB stars in the field of the 38.8d Cepheid U Carinae indicates that 4 early B stars lying within about 92 pc projected distance of U Car are quite likely to be physically associated with the Cepheid. The derived distance of 1.8 kpc for these stars places them foreground to both Car OB1 and Trumpler 17. Their inferred age of $\sim 18\times 10^6$ years argues that they are unrelated to Trumpler 17.

Field reddening charts for the fields of U Car and Trumpler 17 are presented. The derived space reddening of E(B-V)=0.30 ±0.03 for U Car confirms the recently published photometric reddening for this variable. The field reddening of Trumpler 17 reveals its core region to be relatively free of dust, as has been found by other authors for various other young clusters.

List of Figures

List of Tables

I   Introduction

It has been nearly 75 years since Henrietta Leavitt (1912) first deduced the existence of the Period-Luminosity (P-L) Law for Cepheid variables in the Small Magellanic Cloud. This was surely one of the most significant astronomical discoveries of the present century and it is appropriate here to include some detail on this early work to serve as background for what is to follow. Fernie (1969) provides an historical review of this topic and much of the following discussion is taken from his paper.

The first attempts to calibrate the Cepheid P-L relation were the independent efforts of Russell (1913) and Hertzsprung (1913) using the method of statistical parallax. However, it is with the name of Harlow Shapley (1918) that the development of the P-L Law is inextricably linked. It is now widely appreciated that early work on the P-L relation suffered from the failure to distinguish between what have since come to be known as Population I and Population (and Type) II Cepheids. However, the details as to how the confusion actually arose are generally misunderstood even within the astronomical community.

Prior to progressing further we digress briefly to describe the physical characteristics of these two varieties of Cepheids as well as those of their less-luminous horizonal branch analogues, the RR Lyrae variables. All are, of course, stars whose light output varies as a result of pulsationally unstable atmospheric envelopes. Cepheids are yellow supergiants with spectral types ranging from F through K. The massive, young and metal-rich Population I Cepheids are distinguished from their lower mass, older and (generally) metal-poor Population II and Type II counterparts by being intrinsically more luminous. The Population II and Type II Cepheids are a somewhat inhomogeneous group, although they all appear to represent low-mass suprahorizontal and asymptotic branch stars with a range of metallicities. The period ranges of these two classes overlap considerably from ~1 to 70 days. The shorter period RR Lyrae stars are old, low mass, metal-poor giants of spectral type A. These are very short period [<1 day] variables exhibiting uniform intrinsic luminosities independent of period. Thus, all RR Lyrae variables have very nearly the same mean absolute magnitude [<Mv>=0.6].

As chronicled in Fernie's review, Shapley's original calibration was based on 11 Cepheids. It must be emphasized that the existence of distinct stellar populations was not the only unappreciated fact serving to confound

researchers during the early years of this century. The effects of interstellar extinction, while suspected, had not been quantitatively formulated. The 11 Cepheids used in Shapley's calibration were, in modern terms, Population I objects. As such they were of low galactic latitude and thus significantly affected by the dust layer in the plane of the Galaxy. Shapley's calibration, based on the method of statistical parallax, was also adversely affected by the influence of galactic rotation on the radial velocity and proper motion data. These two factors, when combined with the sparse quantity and poor quality of the data available to Shapley, caused him to underestimate the mean luminosity of his 11 Cepheids by 1.4 magnitudes. Thus, the notorious 1.5 magnitude discrepancy that effectively 'doubled the size and age of the known universe' when announced in 1952, had been incorporated into the very earliest calibrations of the P-L Law before Cepheids of Population II had even been considered. It was when Shapley turned his attention to the Cepheids in globular clusters that coincidence intervened to perpetuate an error that was not to be corrected until Baade's landmark studies of the Andromeda Nebula conducted during World War II. Shapley found that the Cepheids in globular clusters, which we now recognize as Population II W Virginis and BL Herculis variables, seemed to fit his calibration well. It is, of course, now known that these

Population II Cepheids are 1.5 magnitudes less luminous than their Population I counterparts, almost exactly the amount of the error in Shapley's calibration introduced by interstellar extinction, galactic rotation and data deficiencies. Shapley accepted this unfortunate coincidence as confirmation that the zero point of his calibration was correct, and proceeded to incorporate the RR Lyrae variables of globular clusters into the relation. His calibration fortuitously predicted a luminosity for these stars close to that accepted today. Thus, when further studies on field RR Lyrae stars verified Shapley's prediction of their luminosity, confidence in his calibration became all but unshakable. Even after Trumpler (1930) firmly established the existence of interstellar absorption, confidence in Shapley's zero-point remained high. It was not until Baade (1952) attempted to fit Shapley's relation to the Cepheids in M31 that incontrovertible evidence against the calibration presented itself. Shapley's work suggested that RR Lyrae stars should be detected at a magnitude of 22.4 in M31, but Baade, using the new 5-m Hale telescope, found them to be 1.5 magnitudes fainter. Baade (1956) enlarged on his work and established the P-L Law in its present form with separate zero-points for Population I and Population II Cepheids.

During the intervening years refinements to the P-L

Law have been made using cluster main-sequence fitting in
addition to statistical parallax. The calibration has
become especially dependent upon the Population I Cepheids
of the nearby Magellanic Clouds since these galaxies con-
tain many such variables located at a common distance from
the Sun. Before the passage of too many more decades,
space-based instrumentation could foreseeably offer orders
of magnitude improvement in the accuracy of trigonometric
parallaxes. However, until the arrival of such halcyon
days, the most powerful means of calibrating Cepheid lum-
inosities is by deriving distances to the stellar groups
in which they are located. Unfortunately, the long-period
Population I Cepheids, the stars most important in deter-
mining distances beyond the Local Group, are rarely found
in clusters and associations. Thus, the calibration remains
heavily reliant on distances determined for the Magellanic
Clouds. That the topic is complex and in need of further
research is made clear by the fact that Cepheids of the
Large Magellanic Cloud appear to obey a slightly, but sys-
tematically, different P-L relation than their Small Magel-
lanic Cloud counterparts. Opportunities to verify or
refine the high luminosity end of the relationship using
long-period Cepheids located in relatively nearby stellar
groups would, therefore, be most propitious. Any procedure
leading to the detection of clusters or associations con-

taining long-period Cepheids holds promise for refining the calibration with consequent improvement in the accuracy of the extragalactic distance scale. This thesis is concerned with techniques whereby such clusters or associations in the vicinity of long-period Cepheids might be discovered.

Numerous investigators (Kippenhahn and Smith 1969, Tammann 1970, Meyer-Hofmeister 1972) have deduced a theoretical relationship between the period and the age of Cepheids using stellar evolutionary models. Such theoretical period-age relations are sensitive to element abundance and mass loss assumptions in the models. They are further complicated by the fact that each Cepheid crosses the instability strip more than once with a different period at each crossing. Since the evolution of massive Population I Cepheids is fast compared to the main-sequence lifetimes of their precursors, Cepheids of nearly identical ages may have significantly different periods if they are observed at different crossings. For example, periods during first crossings of the instability strip are approximately half those of subsequent crossings. However, first crossings are very fast compared to subsequent crossings and, therefore, are rarely observed. Differences in period between second and subsequent crossings are much less pronounced, permitting the ages of these stars to be determined with an accuracy of 10-15 percent (Kippenhahn and Smith

1969). Thus, the scatter inherent in period-age relations
of long-period Cepheids is sufficiently small to permit
the conclusion that the indicated ages of these stars [<35My
for P>10d] are comparable to the main-sequence lifetimes
of early B stars. It is therefore not unreasonable to
expect that a long-period Cepheid may share a common
physical origin and distance with any cluster or assoc-
iation of young stars found in its immediate vicinity.

van den Bergh and Harris (1976) showed that the
presence of a sparse cluster of B stars (Lyngå 6) surroun-
ding the 10 day Cepheid TW Normae was evident from inspec-
tion of the colour-colour (CC) diagram for the stars in
the variable's vicinity. The CC diagram revealed a con-
spicuous grouping of reddened OB stars near the Cepheid.
In a series of subsequent papers (van den Bergh et al.
1982, 1983, 1984) the fields surrounding 14 long-period
Cepheids were investigated using photographic photometry.
Colour-colour and colour-magnitude (CM) diagrams were
constructed for each field. The rationale of the method
is that any association or cluster of young stars to which
the Cepheid might belong would be evident as a well defined
sequence in the CM plane and as a conspicuous group of
stars with similar reddenings in the CC plane. If such
groupings are detected, spectroscopic studies could be
initiated to further test for membership of the Cepheid

from similarity of radial velocity. Distances to the clus-
ters or associations containing such long-period Cepheids
could then be used to further refine the P-L Law for these
stars, consequently improving the accuracy of the extra-
galactic distance scale. Only 2 of the 14 fields inves-
tigated to date have been sucessful in the sense of deter-
mining that the Cepheid in question is a likely member of
a nearby association. In neither case (CT Car and OO Cen)
have spectroscopic data yet been obtained to confirm or
deny the question (van den Bergh, 1985). In several of
the other fields studied it may be that photometric errors
and insufficiently rigorous analyses have conspired to
obscure the Cepheid-association connections.

This thesis applies a similar but somewhat more sophis-
ticated method of analysis, incorporating differential red-
dening, to search for any related cluster or association
in the vicinity of the 13.2 day Cepheid GT Carinae. In
the course of carrying out the required measurements it
became apparent that a search to fainter magnitudes than
permissible by the available plate material would be neces-
sary. The study was then expanded to include a re-inves-
tigation of the closely adjacent fields surrounding the
open cluster Trumpler 17 and the 38.8 day Cepheid U Carinae.
The field of U Car was investigated previously by van den
Bergh et al. (1984) who were unable to find evidence for

any related cluster or association in its vicinity. Since previous studies of Trumpler 17 indicated this cluster to be at a distance comparable to U Car, it was felt that a more detailed investigation into a possible cluster-Cepheid association would be worthwhile.

Other clusters of interest lying within the field of the photographic plates include Pismis 17, Hogg 9 and Feinstein 1, but they could not be studied using only the plates available. Future study of these clusters would also be worthwhile to investigate their possible association with U Car.

II Observational Data

(a) Plate Material

The plate material used for this study consists of 2 U band plates and one each in B and V obtained between 1978 and 1982 by E. Brosterhus and F. Younger with the 1.0 metre Swope telescope in Chile at the Las Campanas Observatory of the Carnegie Institution of Washington. The plates were centered on GT Carinae (R.A. 10^h 57^m 22^s dec $-59°12'.9$ 1950) which lies approximately midway between the Eta Carinae nebula and the populous young cluster NGC 3532. A plate journal is included in Table I.

Table I

Photographic Plate Data

Plate	Date UT	Emulsion	Filter	Exposure (min)
CF2610	1982.02.25	103a-D	GG495	30
CF2615	1982.02.26	103a-O	UG1	90
CF1982	1978.05.12	103a-O	UG1	68
CF2108	1979.03.31	103a-O	GG385	30

(b) Photoelectric Data

Skeleton photoelectric observations (one obser-

vation per star) of sequences surrounding U Car and GT

Car from van den Bergh et al. (1984) and van den Bergh

(unpublished) are listed in Tables II and III. An addit-

ional 5 photoelectric observations in the vicinity of Trum-

pler 17 from Sher (1964) are given in Table IV.

Table II

U Car Region Standards

Photoelectric data are from
van den Bergh et al. 1984.

Star	Photoelectric			:	Photographic		
	V	B-V	U-B	:	V	B-V	U-B
A	11.00	1.97	1.84	:	10.81	1.85	1.48
B:	13.03	0.63	0.18	:	13.06	0.59	0.06
C	12.13	0.15	0.04	:	12.05	0.17	0.09
D:*	13.02	0.48	0.23	:	13.00	0.51	0.31
E	13.91	0.52	0.06	:	13.87	0.49	0.07
F:	13.53	0.41	0.08	:	13.55	0.46	0.06
G	15.51	0.66	0.34	:			
H	16.65	0.56	....	:			

: Stars used for calibration and transformation as
discussed in the text.

* Vpe adjusted from 13.32. See text.

Photographic values from equations (1) through
(3) are given for stars lying on the linear por-
tions of Figures VIII through XI. See Section III.

A detailed discussion of the photoelectric observations

is deferred to the following section. The stars in these

sequences are identified on the V band finder charts given

in Figures 1, 2 and 3. Note that standards 59 and 60 in

Table III

GT Car Region Standards

Photoelectric data are from van den Bergh (unpublished).

Star	Photoelectric			:	Photographic		
	V	B-V	U-B	:	V	B-V	U-B
A	8.29	0.02	-0.03	:			
B:	10.92	0.20	-0.78	:	10.96	0.17	-0.75
C	12.47	0.32	-0.04	:	12.50	0.62	-0.18
D:	12.84	0.35	0.13	:	12.84	0.32	0.23
E.	11.65	1.44	1.56	:	11.25	1.56	1.18
F:	13.09	0.65	0.21	:	13.15	0.49	0.20
G:	13.18	1.27	0.98	:	13.02	1.22	0.61
H	13.63	0.33	0.22	:			
I	15.17	1.27	....	:			

Table IV

Trumpler 17 Standards

Photoelectric data are from Sher (1964).

Star	Photoelectric			:	Photographic		
	V	B-V	U-B	:	V	B-V	U-B
4:	12.46	0.41	-0.28	:	12.51	0.47	-0.21
5:	11.28	0.47	-0.15	:	11.26	0.50	-0.10
57	11.49	1.04	0.79	:	11.50	1.05	0.40
59*	9.88	0.06	-0.04	:			
60*	11.64	0.33	-0.20	:	11.75	0.28	-0.18

The V magnitudes shown in Table IV have been increased by 0.08 over the values in Sher (1964). See Section III for a discussion.

: In both Table III and Table IV denotes stars used for calibration and transformation as discussed in the text.

* Mistakenly identified in Sher (1964). See text

Photographic values in both Table III and Table IV, from equations (1) through (3), are given for stars lying on the linear portions of Figures VIII through XI. Details are given in Section III.
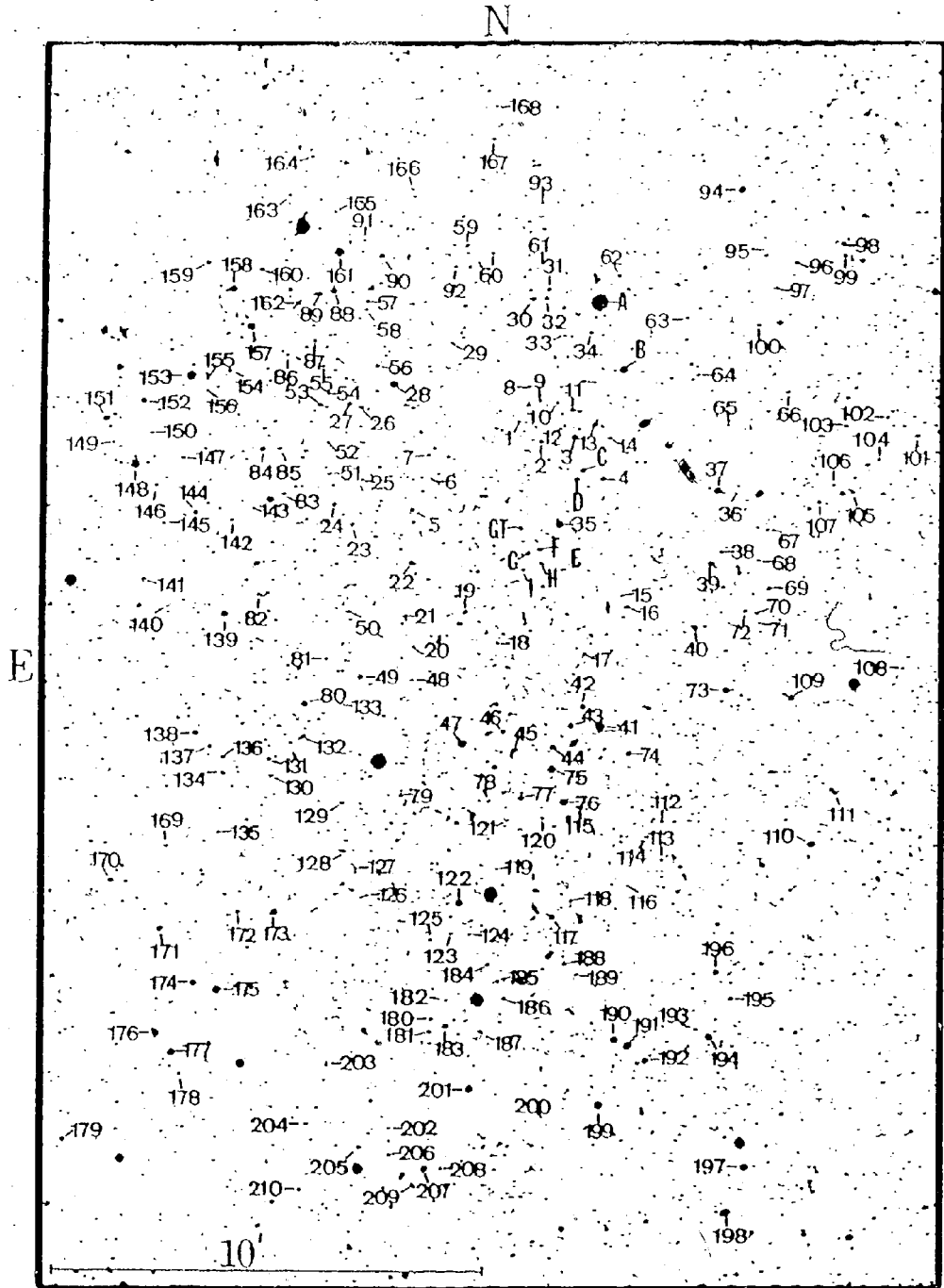
Figure 1

Finder Chart in Visual Light for GT Carinae Field
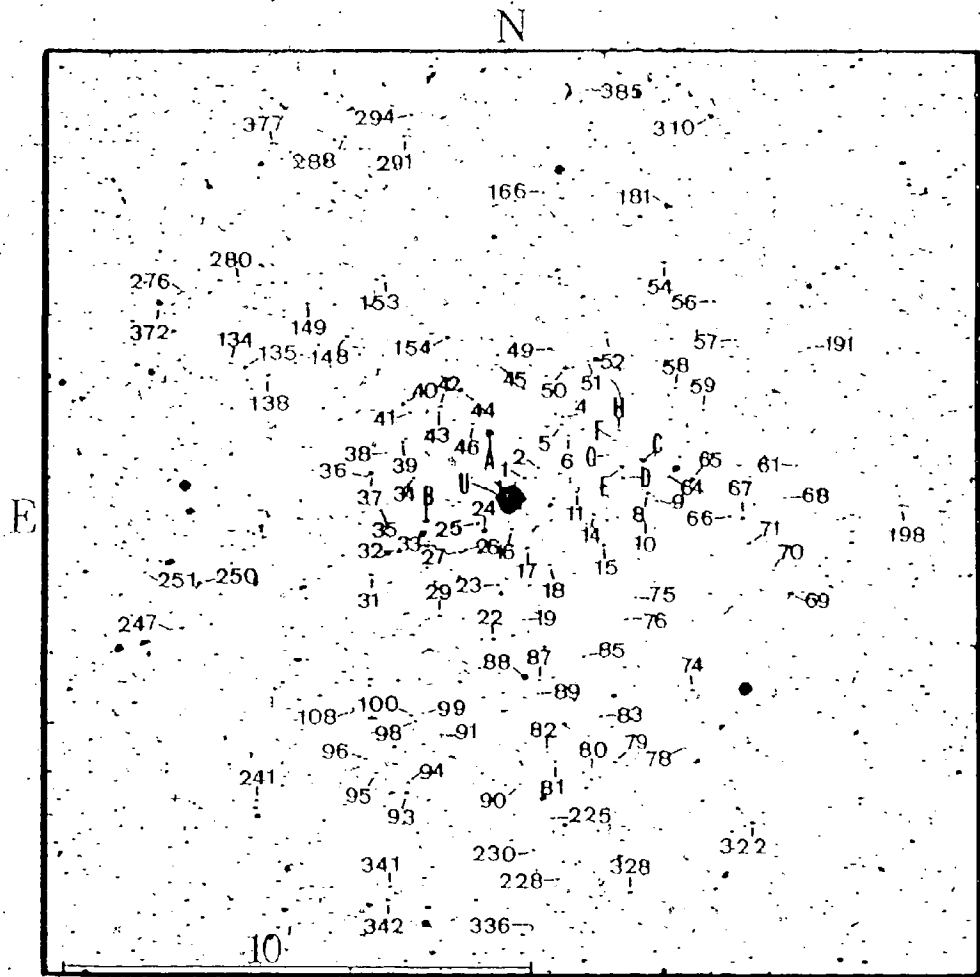
Figure 2

Finder Chart In Visual Light for U Carinae Field

Star numbering is from van den Bergh et al. (1984)
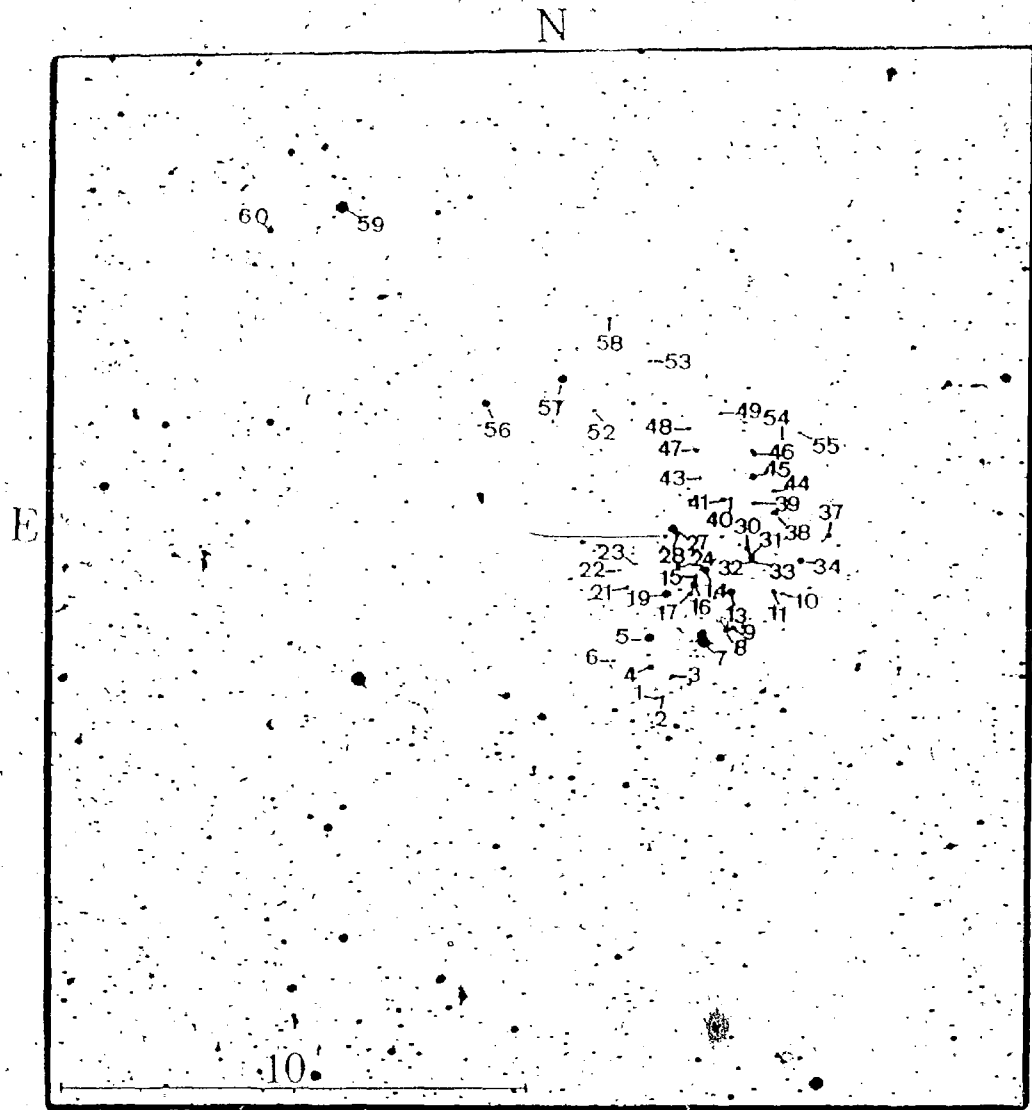
Figure 3

Finder Chart in Visual Light for Trumpler 17 Field

Star numbering is from Sher (1964)

the field of Trumpler 17 were found to be mistakenly iden-
tified in the finder chart published by Sher (1964). A pair
of stars, approximately 2' northeast of the images ident-
ified as 59 and 60 by Sher, and lying outside of his chart,
were found to provide a much better fit to the photo-
electric data. It is these two stars that are correctly
identified as stars 59 and 60 in Figure 3. A line drawing
indicating the positions of U Car and Trumpler 17 relative
to GT Car within the field of the photographic plates is
given in Figure 3a.
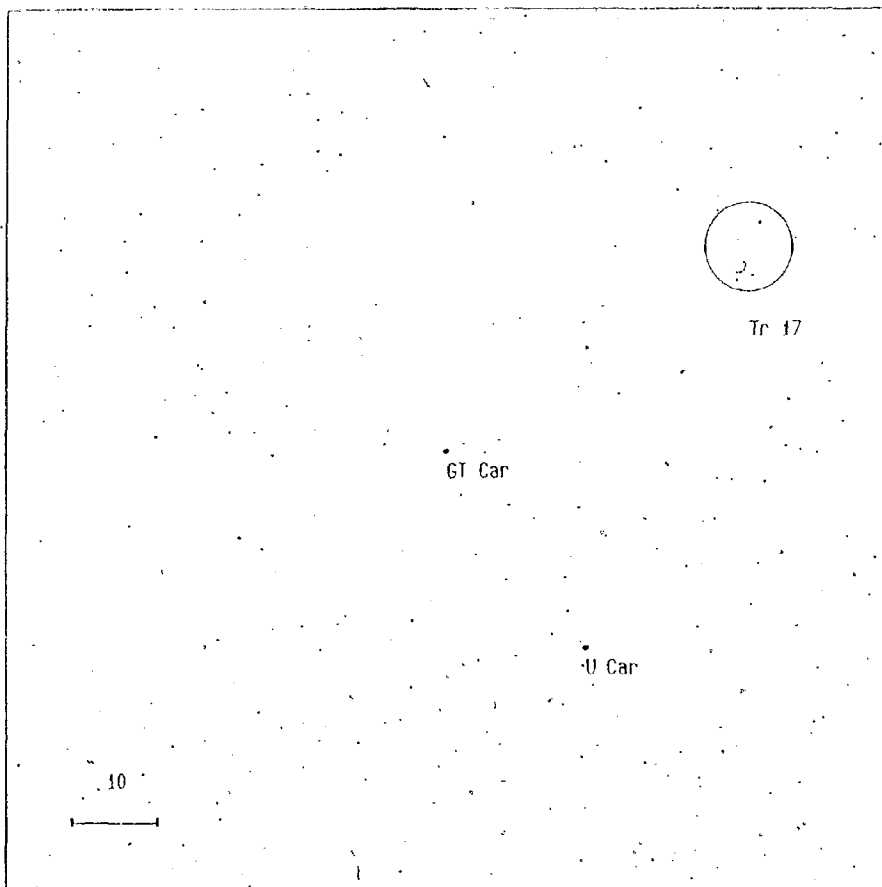
Figure 3a

Relative Field Positions

Relative positions within the field of the
photographic plates are indicated for the
Cepheids GT Car and U Car as well as for
the cluster Trumpler 17.

III Plate Calibration and Transformation Parameters

(a) Scatter in the photoelectric data

At the outset of irising, it became evident that objectionably large scatter existed in the photoelectric data. A plot of the square of the iris readings versus unadjusted photoelectric B magnitudes for all standards measured, following the method of Schaefer (1981), is given in Figure 4. Standard GT Car/A was too bright to be measured on all plates and does not appear. The repeatability of the photographic measures was excellent and the standards selected for calibration and transformation did not suffer from crowding by neighbouring star images.

Prior to adopting the I^2 versus magnitude relation suggested by Schaefer (1981), tests were conducted for the linearity of I^n versus magnitude for values of n ranging from 1 to 5. Correlation factors from these tests indicated no advantage was to be gained in using higher powers of I than the second.

The iris values plotted in Figure 4 are the average of 3 readings obtained at separate measuring sessions, a method followed for all subsequent calibration plots as

Figure 4

Plate CF2108: Unadjusted photoelectric values
for all B standards In Tables II, III and IV.
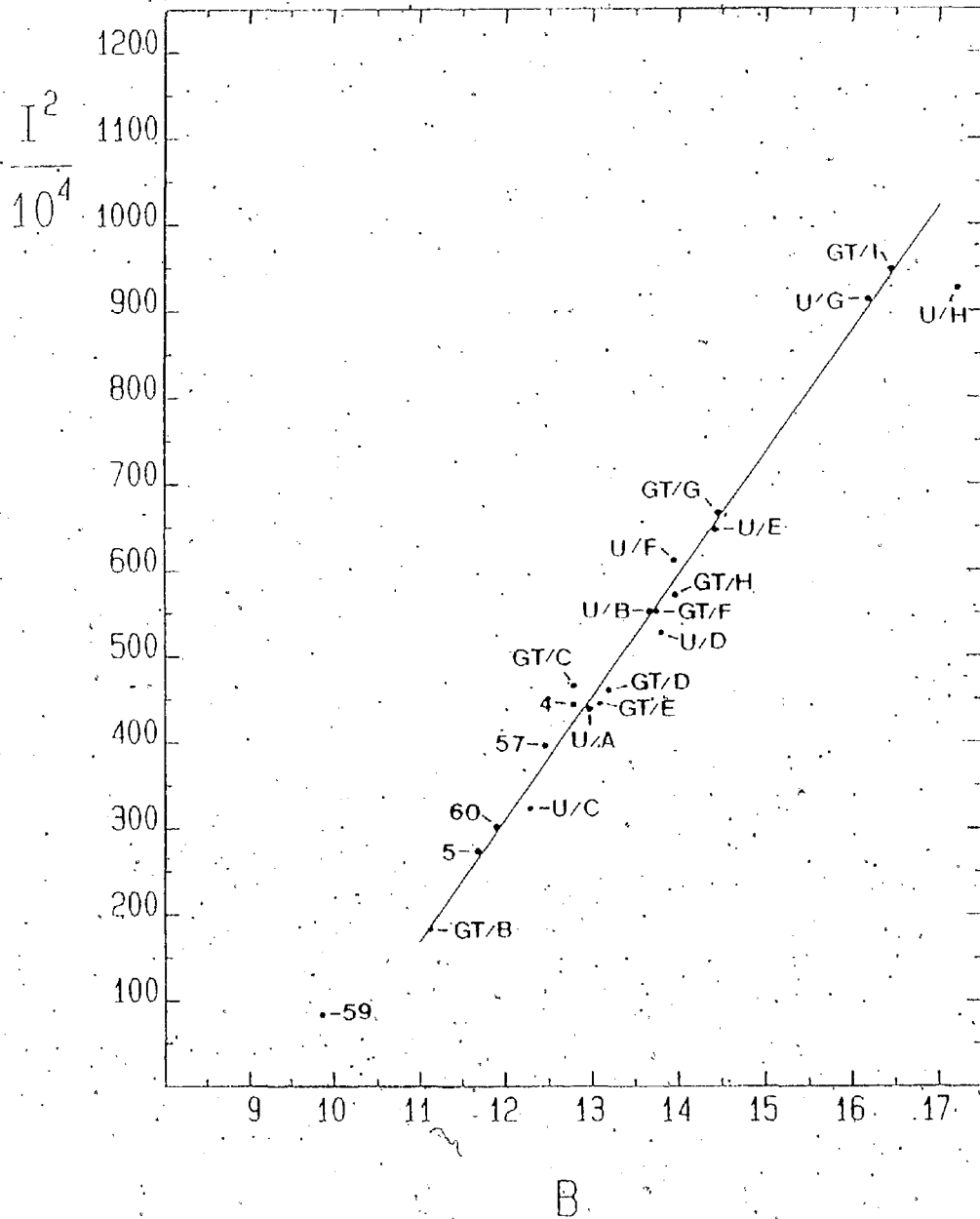
well. Care was taken to ensure that the same instrument

set-up was used at each session by setting on a standard

of intermediate brightness and adjusting the photometer

for an identical iris reading at null. The straight

line shown is a least squares fit to the photoelectric

data over the range in B indicated (11.00-17.00). The

standard deviation of the least squares fit is ±0.24 mag

in B. Due to the scatter in Figure 4, especially for stars

U Car/F and GT Car/H, and the clustering near B=13.00, the

transformation equations derived from the entire set of

standards also exhibited excessive scatter with standard

deviations of ±0.12 mag in V, ±0.10 in B-V and ±0.14 in

U-B. The photoelectric data for the GT Car and U Car field

sequences are the result of single observations for each

star, as stated by van den Bergh et al. (1982, 1983). Thus,

the existence of the scatter in Figure 4 should not be con-

sidered surprising, since it can readily be explained by

the accidental inclusion of a few variables or discordant

observations in the photoelectric sequence. It should

be noted that the plates used in this study were exposed

at substantially different epochs (Table I). Thus, the

inadvertent inclusion of variable stars can be expected

to produce spurious colours for such objects. This point

is significant not only for the present discussion of

calibration and transformation standards but also for the

interpretation of CC and CM diagrams in following sections.

In order to derive calibration plots and transformation equations exhibiting reasonable scatter, it was necessary to select a subset of the standards listed in Tables II, III, and IV. As no attempt was made to measure stars as faint as U/H or as bright as 59 on any plate, their deviation from the linear relation shown in Figure 4 is of no concern and these stars were excluded from further consideration. Standard GT/E, an elongated image on the B plate and a clear multiple image on both U plates, was also rejected. Standard U/D was adjusted in V by -0.30 mag, thereby yielding results more consistent with other standards in all calibration plots as well as in the transformation plots discussed in section (c). It seems likely that the magnitude cited for this star in van den Bergh et al. (1984) was erroneously transcribed prior to publication and not noticed subsequently.

Figure 4 suggests the possibility of a systematic error in the photometry of Sher (1964) for the Trumpler 17 photoelectric sequence. All 5 of the stars in the sequence were found to be overly bright when compared to the linear relation shown, despite their use in obtaining this relation. Moffat (1974), using the photometry in Sher's paper, found a similar systematic error in Sher's observations of NGC 3603. An increase of 0.08 in the V

magnitudes published by Sher, an adjustment advocated
by Steppe (1977), resulted in a better fit to the rest
of the photoelectric data for both the calibration and
transformation relations.

The nine stars finally selected for purposes of plate
calibration and transformation to the UBV system fol-
lowing this involved winnowing process are indicated by
colons in Tables II, III and IV.

(b)   Calibration Plots

Plots of the square of the iris reading versus
photoelectric magnitude for the selected subset of stan-
dards are shown in Figures 5 through 8.   In each case a
straight line, fitted by the method of least squares, is
shown over the approximate range of magnitudes actually
measured on each of the four plates.   It is seen from
Figures 7 and 8 that the B and V band calibration plots
are extended 1.0 to 1.5 magnitudes beyond the brightest
and faintest of the photoelectric standards used in their
construction. The justification for this procedure is dis-
cussed by Schaefer (1981). Schaefer has found a 6 magnitude
range of linearity to be typical of photographic emulsions,
and this is supported by the results of other work at Saint
Mary's University. The adjustment of several of the photo-

Figure 5

Plate CF2615 Calibration
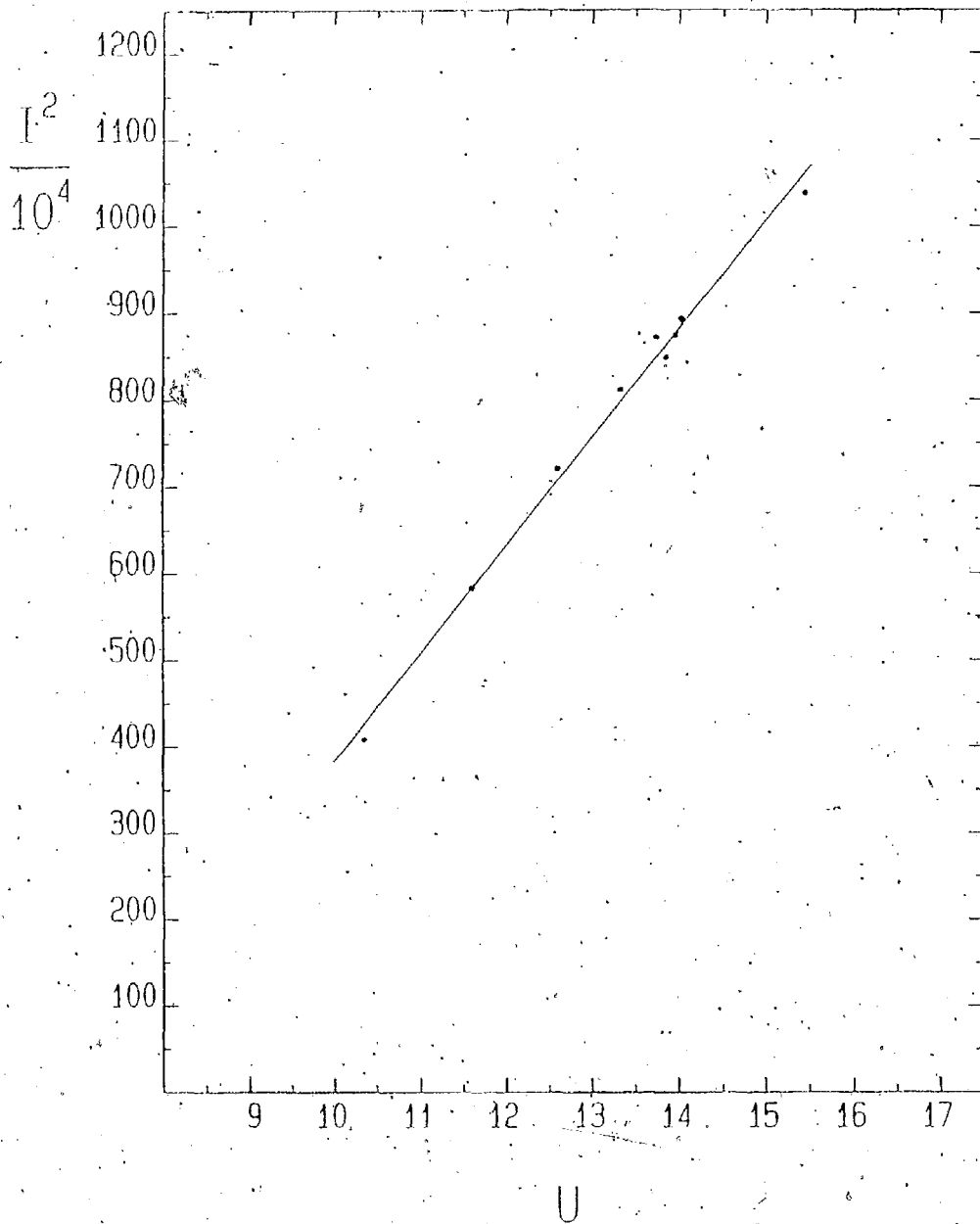
Figure 6

Plate CF1982 Calibration
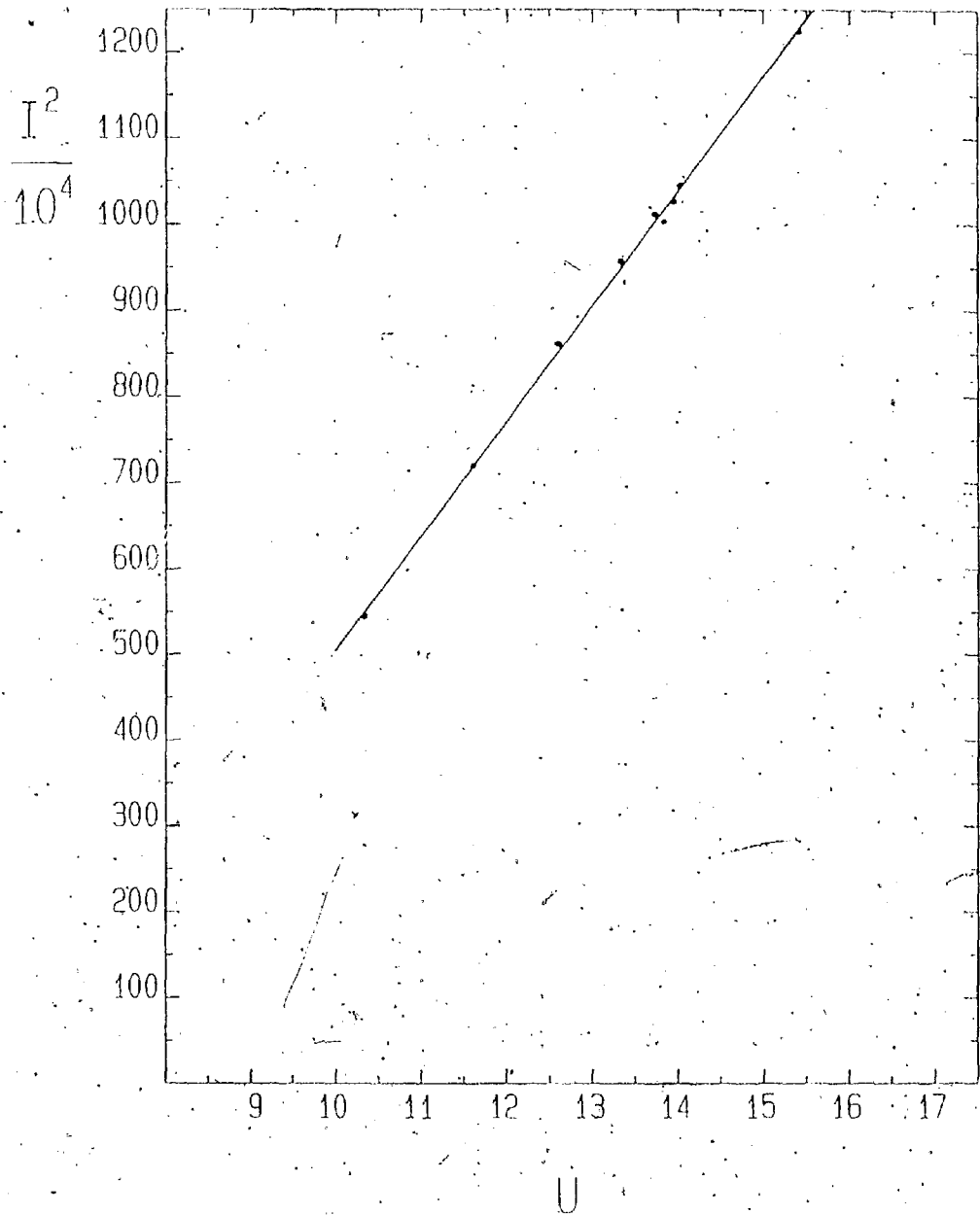
Figure 7

Plate CF2108 Calibration
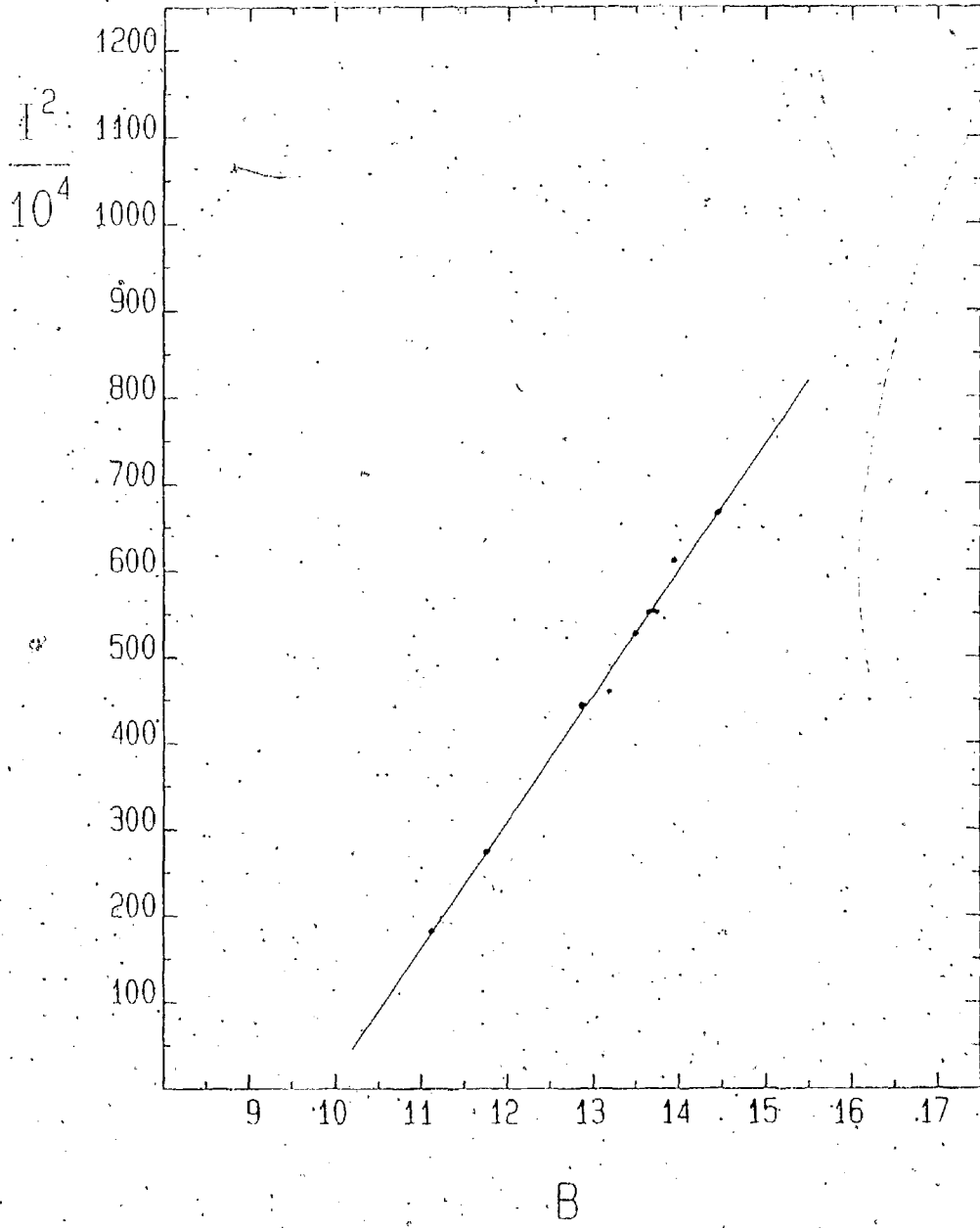
Figure 8

Plate CF2610 Calibration
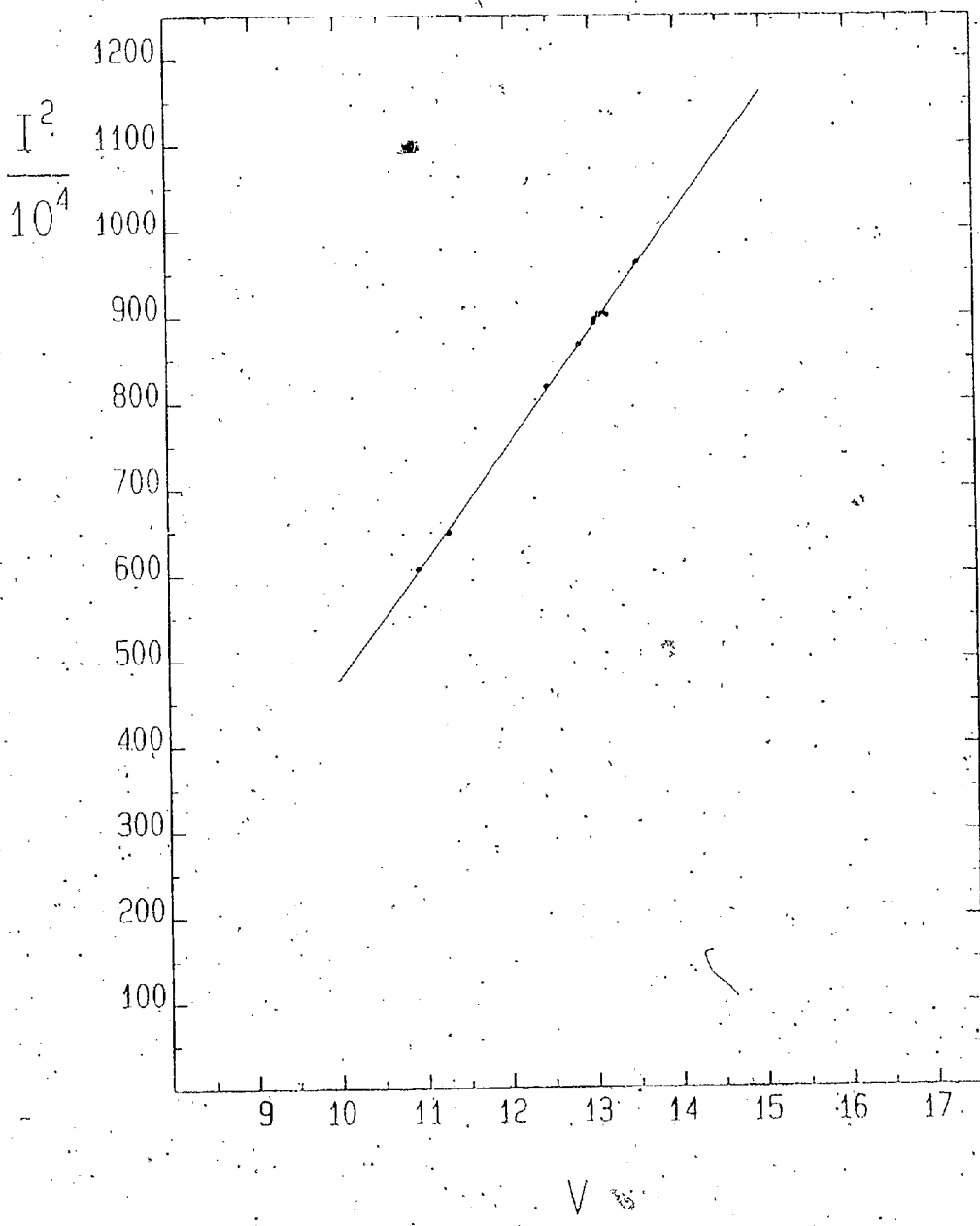
electric standards and the elimination of others, as dis-
cussed in the previous section, had the effect of sig-
nificantly reducing the scatter about the derived trans-.
formation relations, but had only minor influence on the
slope/intercept parameters.   This is evident from a com-
parison of Figures 4 and 7.   The relation of Figure 7,
used to obtain instrumental B magnitudes, is virtually
identical to that of Figure 4, which is defined at the
bright end by standard GT/B and at the faint end by
both GT/I and U/G.   Thus, the relation of Figure 7 is
not as poorly anchored at its extremes as first appears.
Similar remarks apply to the case of the V plate calib-
ration of Figure 8.

(c)   Transformation Relations

Instrumental magnitudes, u, b and v, obtained from
the relations shown in Figures 5 through 8, were trans-
formed to the UBV system using equations of the form:

$$V - v = A(1) \times (b-v) + B(1) \qquad (1)$$

$$B - V = A(2) \times (b-v) + B(2) \qquad (2)$$

$$U - B = A(3) \times (u-b) + B(3). \qquad (3)$$

The fitted relations are shown in Figures 9, 10 and
11, while slope/intercept parameters and errors are
listed in Table V.   The straight lines shown are least
squares fits to the data over the approximate ranges in

Figure 9

Transformation Plot No. 1

Straight line shown is a least squares fit to the data over the approximate range in b-v values actually measured.
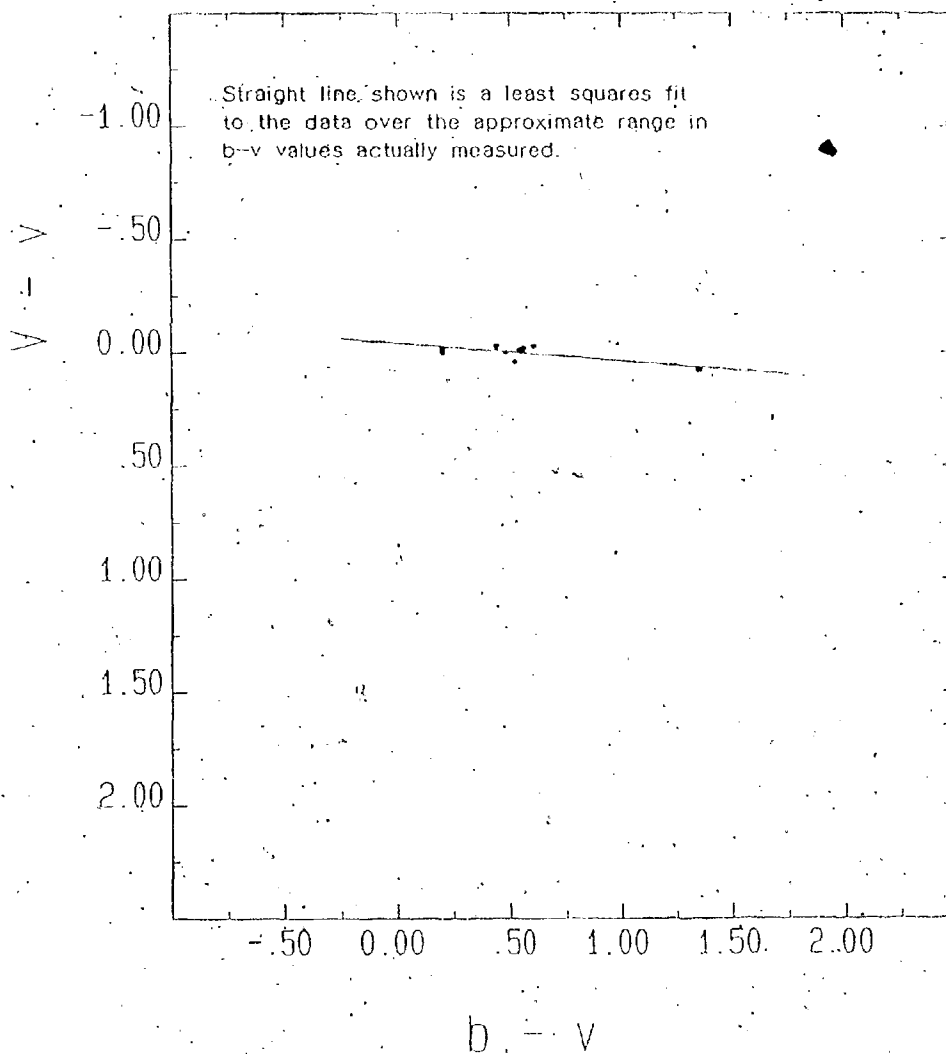
Figure 10

Transformation Plot No. 2

Straight line shown is a least squares fit
to the data over the approximate range in
b-v values actually measured.
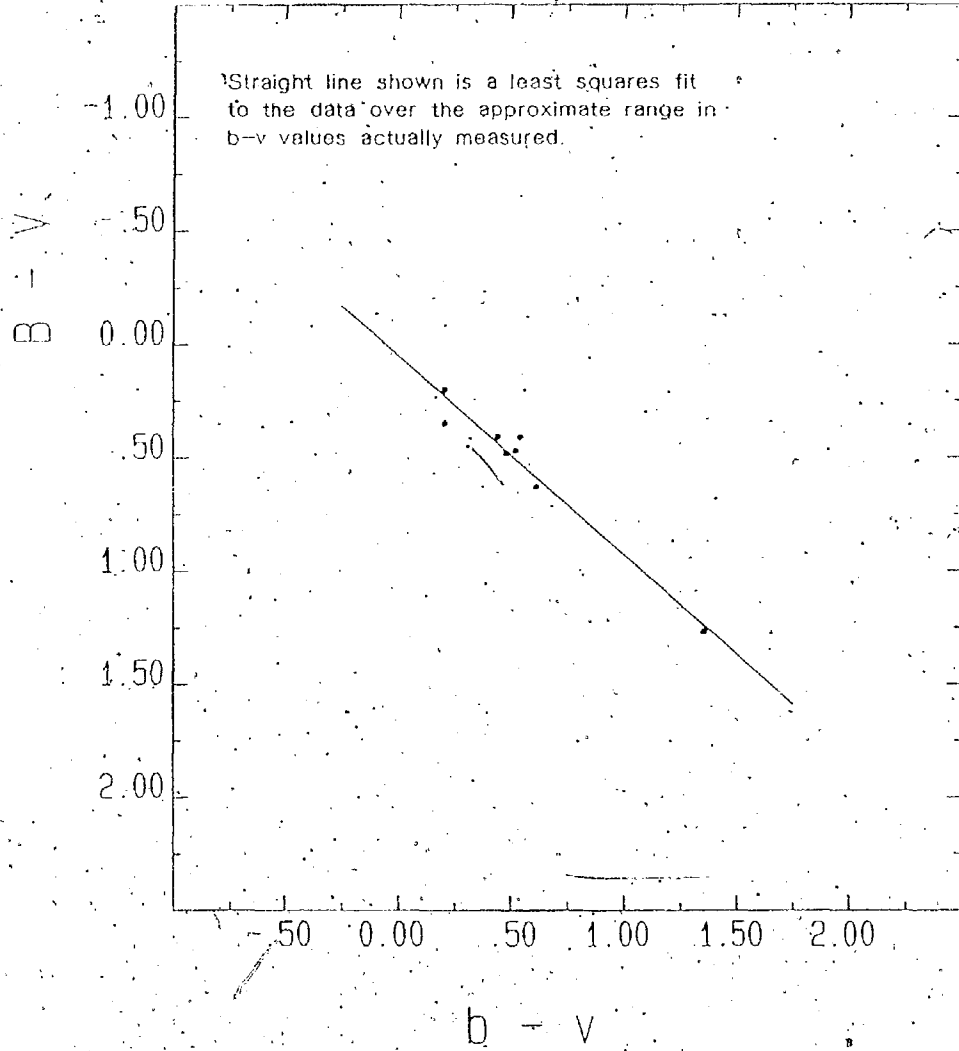
Figure 11

Transformation Plot No. 3

U – B

Straight line shown is a least squares fit
to the data over the approximate range in
u–b values actually measured.

u – b
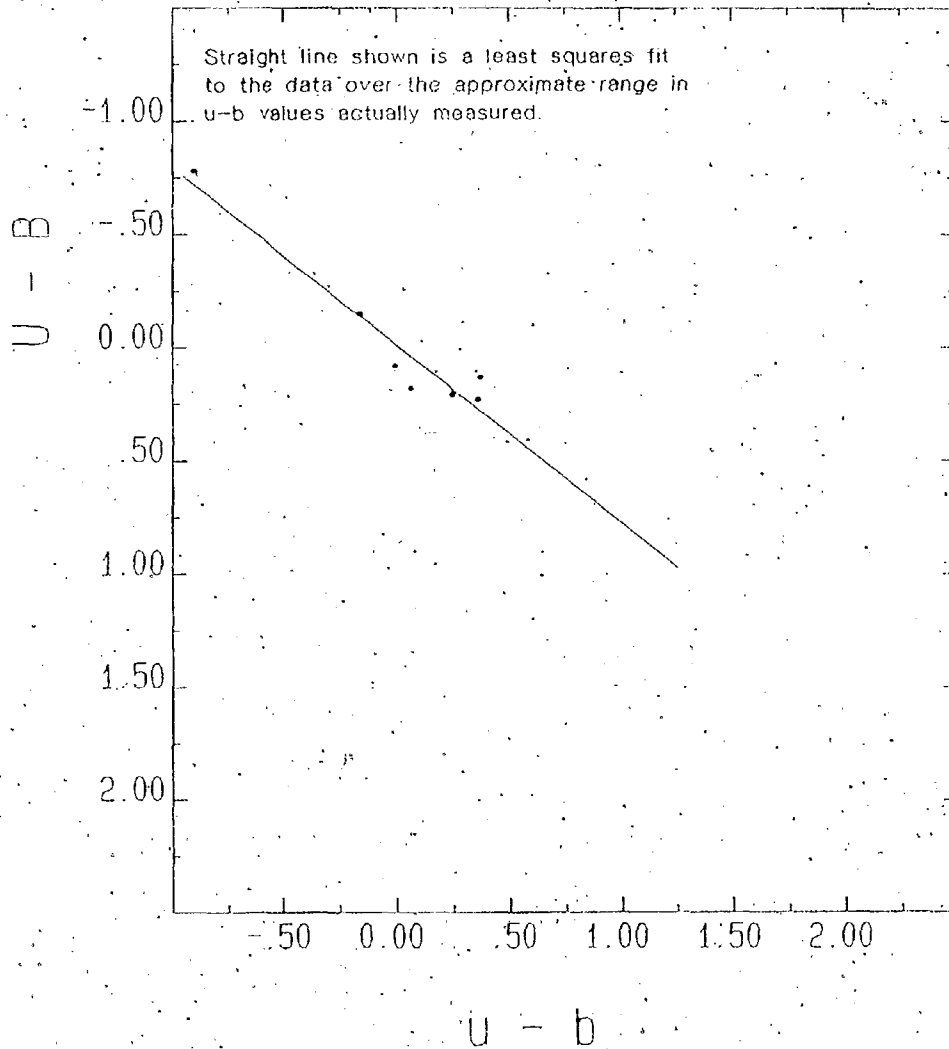
Table V.

Transformation Parameters

Equation	A		B	
(1)	0.079	±0.028	−0.042	±0.018
(2)	0.88	±0.079	0.051	±0.051
(3)	0.79	±0.100	−0.010	±0.041

instrumental colours actually measured. Equations (1),
(2) and (3), with the parameters of Table V yield sample
standard deviations of ±0.03 mag in V, ±0.07 mag in B−V
and ±0.10 mag in U−B for the photoelectric standards used
in their derivation. These measures of dispersion will
be used as error bars in the CC and CM diagrams const-
ructed from data reductions using equations (1) through
(3). Photographic magnitudes and colours for standard
stars lying on the linear portions of the calibration
plots (Figures 8 through 11) are included in Tables II,
III and IV.

The possibility of an undetected systematic error
in U−B for very red stars is evident from Figure 11.
No star of (U−B)>0.25 was included in the subset of photo-
electric standards selected for calibration and trans-
formation purposes. This is not serious as the methods
of analysis used in subsequent sections rely mostly on
early-type stars of (U−B)<0.25 mag.

IV GT Carinae Field

(a) Data Sample

As one of the goals of the study was to search for
any cluster or association of young stars in the vicinity
of GT Car, blue stars near this Cepheid were preferen-
tially selected for measurement. Initially 400 stars
within approximately 10' of GT Car were measured on
U plate CF2615. The B plate was deeply exposed and of
the 400 stars measured on plate CF2615, only about 300
were sufficiently free from crowding problems to be
measurable on plate CF2108. Elimination of stars both
too bright and too faint to fall on the linear portion
of the calibration plots further reduced the data sample
to 210 stars. Transformed V magnitudes and colours
for these stars are listed in Table VI. The stars
are identified on the V band finder chart given in
Figure 1.   A careful examination of the finder chart
raises questions as to the completeness of the photo-
metric survey. There are knots of stars within a few
arc minutes of the Cepheid which were precluded from
study by crowding problems. Conspicuous groupings (pos-
sible faint clusters) ~ 3' west and ~ 1 1/2' northeast are

Table VI

Stars in GT Carinae Field

Star	V	B-V	U-B
1	13.75	0.33	0.32
2	13.77	0.53	0.01
3	12.48	1.37	0.80
4	12.79	0.27	-0.15
5	13.75	0.46	-0.01
6	14.27	0.61	0.09
7	13.88	0.39	0.17
8	13.59	0.16	-0.19
9	14.32	0.32	0.15
10	13.99	0.48	0.20
11	13.06	0.12	0.03
12	14.24	0.33	0.19
13	13.55	-0.01	0.39
14	14.09	0.46	0.04
15	14.00	0.50	0.19
16	13.34	0.95	0.38
17	14.04	0.38	0.25
18	13.01	0.07	0.23
19	13.38	0.54	0.14
20	14.06	0.30	0.16
21	13.69	0.61	0.29
22	12.95	0.22	0.06
23	13.89	0.47	0.08
24	13.70	0.49	-0.06
25	14.44	0.29	0.14
26	13.25	0.34	0.15
27	13.29	0.04	0.29
28	11.27	1.44	1.20
29	13.55	0.12	-0.12
30	12.43	0.24	-0.28
31	13.26	0.03	0.55
32	13.33	-0.09	0.12
33	14.23	0.27	0.15
34	14.28	0.12	0.39
35	13.95	0.63	0.16

Table VI continued

Star	V	B-V	U-B
36	14.28	0.44	-0.05
37	11.33	0.67	0.32
38	13.90	0.68	0.17
39	12.64	0.10	0.28
40	12.53	0.17	0.28
41	10.68	1.43	0.83
42	12.94	0.49	0.01
43	12.94	0.04	0.17
44	12.40	0.37	0.16
45	12.92	0.43	0.43
46	12.73	0.54	-0.02
47	11.36	1.28	0.41
48	14.16	0.49	-0.34
49	12.35	1.13	0.50
50	13.35	0.45	0.16
51	13.95	0.27	-0.14
52	13.99	0.38	0.07
53	12.85	-0.07	0.43
54	13.69	-0.06	-0.05
55	14.59	0.19	-0.09
56	13.51	-0.03	-0.04
57	13.54	0.42	0.17
58	14.22	0.10	0.28
59	13.35	0.09	0.34
60	14.10	0.55	-0.13
61	13.55	0.45	0.02
62	13.91	0.28	0.12
63	14.49	0.35	-0.31
64	14.12	0.53	-0.23
65	13.90	0.41	-0.39
66	14.07	0.52	-0.47
67	13.84	0.58	-0.01
68	13.85	0.53	-0.11
69	12.71	0.20	-0.25
70	12.88	0.28	0.33

Table VI continued

Star	V	B-V	U-B
71	14.23	0.48	0.28
72	13.60	0.49	0.00
73	11.80	0.12	-0.17
74	12.51	0.34	0.04
75	11.05	0.21	-0.65
76	11.06	0.26	-0.58
77	12.30	0.15	-0.07
78	13.42	0.15	0.19
79	13.89	0.32	0.23
80	12.25	0.42	0.32
81	13.51	0.43	-0.03
82	13.71	0.50	-0.14
83	14.29	0.40	0.17
84	12.74	0.15	0.20
85	14.31	0.36	0.01
86	14.46	0.31	-0.08
87	14.08	0.33	0.26
88	12.00	0.01	0.17
89	12.42	-0.04	0.40
90	11.98	0.74	0.53
91	14.21	0.60	0.00
92	14.21	0.46	-0.02
93	13.25	0.33	0.05
94	11.06	0.42	-0.02
95	13.64	0.62	0.02
96	12.89	0.63	0.09
97	13.45	0.52	-0.02
98	12.84	0.01	-0.22
99	14.15	0.48	0.02
100	13.98	0.47	0.08
101	13.13	0.23	0.09
102	14.04	0.57	-0.01
103	13.32	0.38	0.22
104	13.94	0.17	0.03
105	13.44	0.41	0.19

Table VI continued

Star	V	B-V	U-B
106	14.39	0.79	-0.12
107	13.89	0.62	0.22
108	13.76	0.40	0.24
109	11.54	0.34	0.05
110	11.84	1.33	1.07
111	13.29	0.00	0.46
112	14.01	0.24	0.14
113	14.05	0.69	0.24
114	14.42	0.45	0.14
115	14.17	0.05	0.18
116	14.37	0.52	-0.14
117	12.30	0.45	0.30
118	13.89	0.35	0.28
119	14.42	0.54	-0.04
120	14.26	0.77	-0.02
121	14.14	0.53	-0.01
122	11.55	1.75	1.22
123	14.38	0.35	0.08
124	14.33	0.58	-0.04
125	14.21	0.36	-0.06
126	13.69	0.01	0.37
127	13.95	0.47	0.02
128	13.54	0.02	0.23
129	12.92	0.44	0.04
130	13.64	0.39	0.01
131	13.57	0.20	0.09
132	13.22	0.15	0.28
133	13.93	0.74	-0.06
134	13.21	0.44	0.25
135	14.33	0.39	0.11
136	13.85	0.17	-0.08
137	13.29	0.61	-0.29
138	12.44	0.90	0.34
139	11.72	0.39	0.12
140	14.43	0.40	0.11

Table VI continued

Star	V	B-V	U-B
141	12.72	0.29	0.06
142	14.17	0.45	0.21
143	13.89	0.17	0.01
144	13.31	0.27	0.10
145	13.86	0.36	0.17
146	14.00	0.76	0.20
147	13.62	0.59	0.14
148	10.99	0.13	0.04
149	14.39	0.44	0.13
150	14.03	0.23	0.17
151	11.79	0.55	0.29
152	11.96	1.67	1.18
153	10.40	0.60	-0.10
154	13.13	0.24	0.23
155	14.15	-0.20	0.36
156	14.35	0.66	-0.03
157	11.02	0.09	-0.52
158	11.18	0.05	-0.55
159	12.74	0.13	0.35
160	12.64	1.10	0.51
161	10.70	1.23	0.94
162	12.48	0.39	0.16
163	13.78	0.52	0.02
164	13.63	0.47	-0.03
165	14.46	0.37	0.11
166	14.39	0.59	-0.04
167	14.06	0.27	-0.06
168	13.23	1.14	0.49
169	13.46	0.89	0.21
170	12.46	0.20	0.29
171	12.35	0.66	0.18
172	13.35	0.06	-0.11
173	12.12	0.31	0.36
174	11.80	0.21	0.30
175	10.95	0.90	0.31

Table VI continued

Star	V	B-V	U-B
176	11.31	0.25	-0.16
177	11.40	1.34	0.89
178	14.03	0.73	0.01
179	12.18	0.16	0.24
180	13.86	0.72	0.21
181	13.63	0.76	0.13
182	13.79	0.66	-0.04
183	12.52	0.36	0.05
184	13.35	0.32	0.22
185	13.07	0.21	0.35
186	13.59	0.52	0.22
187	12.95	0.26	0.37
188	12.89	0.30	0.06
189	14.30	0.47	0.11
190	11.41	0.27	0.12
191	11.12	0.21	-0.20
192	11.66	-0.07	-0.25
193	13.00	0.90	0.32
194	11.45	0.31	0.10
195	12.75	1.20	0.60
196	11.78	0.17	-0.03
197	11.04	1.03	0.72
198	11.31	0.22	-0.40
199	11.08	0.40	-0.22
200	13.30	0.34	0.09
201	11.14	0.13	-0.30
202	14.24	0.73	-0.12
203	13.40	0.34	0.15
204	12.96	0.50	0.01
205	13.40	0.27	-0.30
206	13.84	0.60	-0.03
207	12.00	0.16	-0.23
208	14.04	0.54	-0.07
209	13.15	0.46	0.41
210	12.83	0.22	0.25

especially noted. Crowding problems within these groups, evident on the visual light finder chart, were appreciably more severe on the deeply exposed blue plate. Thus, it was not possible to adequately sample such groupings with the available plate material.

(b) Colour-Magnitude and Colour-Colour Plots

CC and CM plots for the GT Carinae field appear in Figures 12 and 13 respectively. In each case error bars represent one standard deviation in colour or magnitude as derived from equations (1), (2) and (3). The ZAMS two-colour relation shown is from Johnson (1966) and a reddening line of slope $E(U-B)/E(B-V)=0.75$, typical of the Carina field (Turner et al. 1980), is included. The existence of stars with "peculiar" colours clustered about $U-B\sim0.25$ and $B-V\sim0.12$ is noted. It is difficult to adequately account for these objects which cannot be dereddened to the standard sequence using any reasonable reddening law. Most may exhibit such colours as a result of photometric error, but ~10 of these stars remain "peculiar" even after adjusting their colours by a full standard deviation in both $U-B$ and $B-V$. A possible explanation is that these are variable stars and their colours, being deduced from plates taken
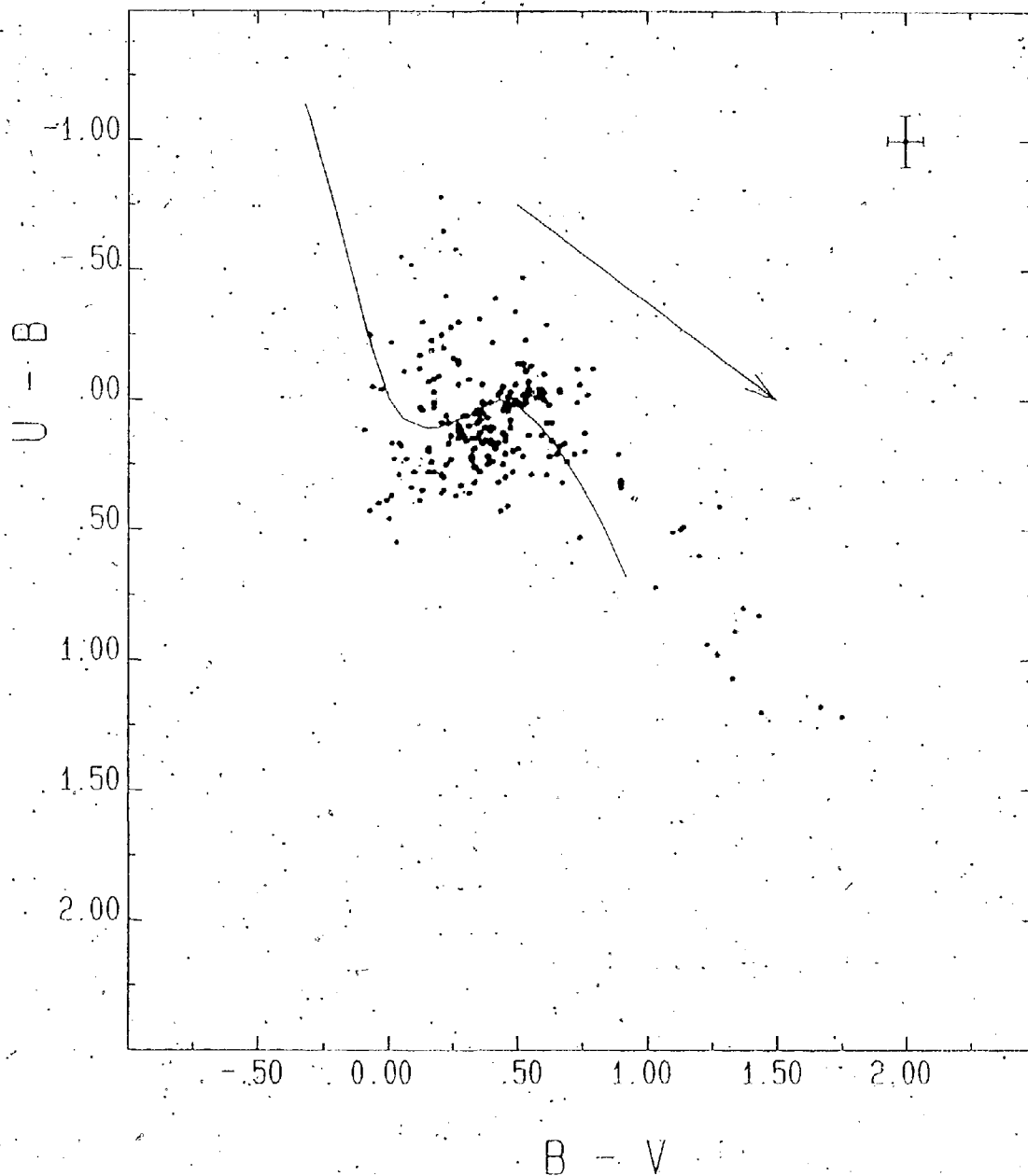
Figure 1.2

CC Diagram for GT Carinae Field

Error bars depicted are for one standard
deviation as explained in the text. ZAMS
relation is from Johnson (1966). A red-
dening line of slope 0.75 is shown.
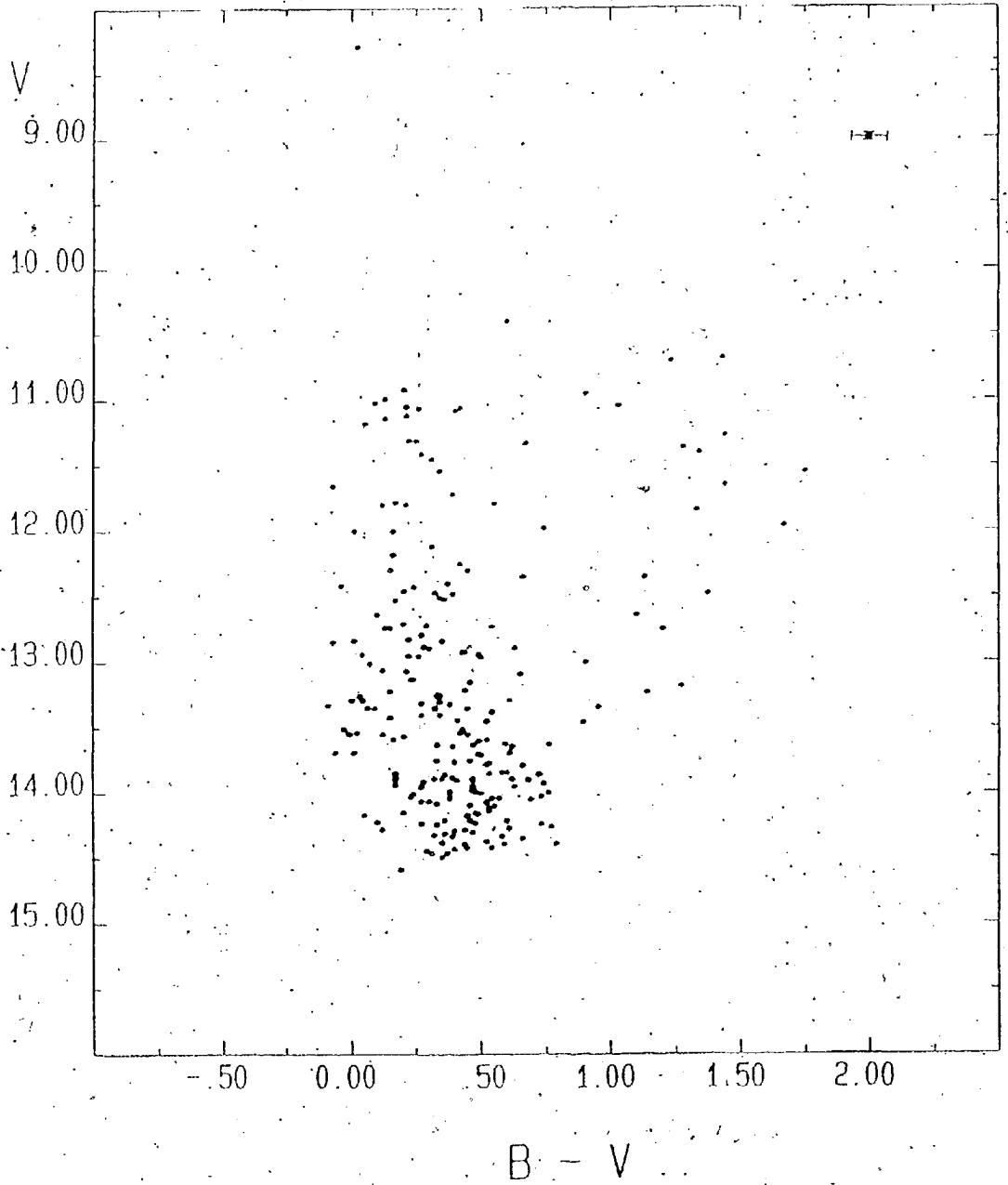
Figure 13

CM Diagram for GT Carinae Field

Error bars depicted are for one
standard deviation as explained in
the text.

at different epochs, are spurious. This supposition is
supported in several cases by comparing magnitudes
derived from the two U plates. Instrumental magnitudes
from these two plates for "peculiar" stars 31, 32 and 159,
for example, differ by 0.25, 0.59 and 0.23 magnitudes.
These are the largest such differences in the 210 star
sample.

No grouping of young stars sharing common reddenings
is obvious from an examination of the two-colour plane.
Also, no well defined main-sequence is detectable from
Figure 13. Thus, within the limits of sample completeness
discussed previously, no immediate evidence for a cluster
or major association of young stars in the vicinity of
GT Carinae is found from these diagrams. However,
differential reddening, which is a relatively common
feature of association fields, can often mask the charac-
teristics of a physical group of stars in such diagrams.
Generally, a more detailed analysis, taking reddening into
account, must be made to search for loose stellar groups
like associations. Such a method of analysis is taken
up in the next sub-section.

(c) Variable Extinction Analysis

It follows from the distance modulus equation that,
for stars at a common distance:

$$V - Mv = C + Av \tag{4}$$

where Av is the total absorption in V and C is a constant
equal to 5 log d -5. The ratio of total to selective
absorption, R, is defined by:

$$R = Av/E(B-V) \tag{5}$$

Thus, a cluster or association will fall along a straight
line in the V-Mv versus E(B-V) plane according to:

$$V - Mv = C + R \times E(B-V) \tag{6}$$

The 23 stars in Figure 12 with (U-B)<-0.12 and (B-V)<
0.50 were dereddened using the reddening line shown. (B-V)o
values obtained were used to derive Mv values for these
stars from the ZAMS relation of Turner (1976). [We shall
consider possible systematic errors introduced into the
analysis from assuming all stars to be ZAMS objects during
discussion of the field surrounding Trumpler 17 in section
V(b).] The Mv data were used to construct the variable
extinction plot given in Figure 14 with the data listed
in Table VII. A solid line of slope R=3.1, represen-
tative of the Carina Field (Turner et al. 1980) is plot-
ted. The zero point of this line at Vo-Mv=12.07 corres-
ponds to the main young stellar group recognized in this
field - the Carina OB1 complex centered on the Carina
Nebula (Feast 1958). Error bars of ±0.39 mag in V-Mv and
±0.02 mag in E(B-V) are depicted. These are estimates of
the errors resulting from the graphical method of obtaining

Table VII

Distance Moduli and Colour Excesses for
Early-type Stars in GT Carinae Field

Star	V – Mv	(B-V)o	E(B-V)
4	12.56	−0.13	0.41
8	13.10	−0.11	0.28
30	12.91	−0.18	0.43
48	15.86	−0.25	0.75
51	13.72	−0.13	0.41
63	15.32	−0.20	0.56
65	15.60	−0.25	0.46
69	12.74	−0.15	0.36
73	11.19	−0.10	0.22
75	14.15	−0.30	0.51
76	13.46	−0.28	0.54
82	14.36	−0.19	0.70
98	12.11	−0.09	0.10
157	12.19	−0.22	0.31
158	12.53	−0.23	0.28
176	11.08	−0.13	0.39
191	11.02	−0.14	0.36
192	10.81	−0.08	0.01
198	12.31	−0.21	0.43
199	11.91	−0.20	0.61
201	11.31	−0.16	0.29
205	14.23	−0.20	0.48
207	11.77	−0.13	0.30

Excesses given are adjusted to an
equivalent B0 star reddening using
equations (9) and (10).

Figure 14

Variable Extinction Plot for GT Carinae Field

A solid line of slope R=3.1 is shown at Vo–Mv=
12.07 corresponding to the distance of the
Carina OB1 nebula complex. A dashed line is
also shown at Vo–Mv=13.40 representing a possible
background association as discussed in the
text. Error bars represent ±0.39 mag in V–Mv
and ±0.02 in E(B–V).

The predicted position of GT Car is also
indicated as discussed in the text.
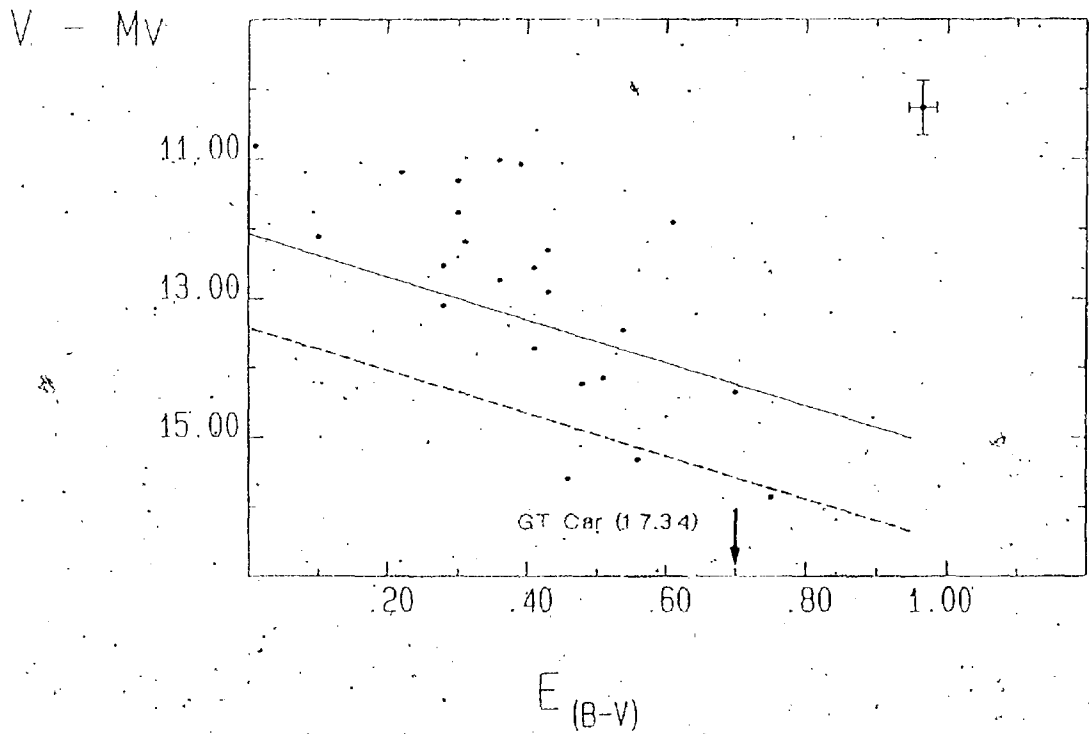
Mv by dereddening stars in the CC diagram to the ZAMS relation. The colour excesses of Table VII and Figure 14 are adjusted to the equivalent reddening of a BO star using equations (9) and (10), as explained later in this section.

Figure 14 is essentially a scatter plot with most of the stars being probable members of Car OB1. A few (3) reddened distant stars are detected with V-Mv>15. They represent members of a more distant background association the existence of which is confirmed by spectroscopic data (see Section VIc). This background group is indicated by the dashed line in Figure 14 at Vo-Mv=13.40 (4.8 kpc).

In order to place GT Car in Figure 14 we make use of the following data for this Cepheid (Madore 1975):

$$<U> = 15.44$$
$$<B> = 14.35$$
$$<V> = 12.91$$
$$P = 13.162d$$
$$\log P(d) = 1.119,$$

where the <> symbols represent intensity means. The use of Madore's data with the period-luminosity and period-colour relations of van den Bergh (1977), namely

$$M<v> = -1.18 - 2.90 \log P \qquad (7)$$

$$[<B>-<V>]o = 0.27 + 0.48 \log P \qquad (8)$$

yields the following predicted values for GT Car:

$$M<v> = -4.43 \quad \pm 0.26$$

$$[<B>-<V>]o = 0.81 \pm 0.06$$

$$E(B-V) = 0.63 \pm 0.06$$

$$V-Mv = 17.34 \pm 0.26$$

Observationally and theoretically it is recognized that stars of widely differing spectral types exhibit different colour excesses when seen through identical amounts of interstellar dust. This is due to the variation of each filter's effective wavelength with spectral type and reddening. To compare GT Car with the field B stars in Figure 14, it is therefore necessary to allow for the intrinsically redder nature of the Cepheid. To do so, the following relations from Fernie (1963) are used:

$$n = 0.97 - 0.09(B-V)o \qquad (9)$$

$$E[B-V](B0) = E[B-V]/n, \qquad (10)$$

yielding an equivalent B0 star colour excess for GT Car of $E(B-V)=0.70$.

It is evident from Figure 14 that GT Carinae is predicted to be too distant for any association or cluster in its vicinity to be detected within the magnitude limits of this survey. It is very likely a background object to our survey stars, being more distant than either the Carina OB1 nebula complex or the more distant group at 4.8 kpc. A line (not shown) of slope R=3.1 drawn through the position of GT Carinae in Figure 14 places the Cepheid at $<V>o-Mv=15.17$, corresponding to a distance of 10.8 kpc!

The data of Figure 14 are also of interest with regard

to the value of R in this region. At various times in the past the region of the Great Carina Nebula has been suggested to contain dust clouds which give rise to anomalous extinction with a value of R near 5 (see Herbst 1976). A similarly steep trend in the data of Figure 14 might lead to the suspicion that stars near GT Car could also be subject to an anomalous extinction law. However, the effects of random errors in the photometry are an important consideration for the present data, and for the stars in question (early B-type) this can produce a systematic scatter in Figure 14 which tends to mimic a large R value (see Garrison 1970, Turner and Moffat 1980). These effects are considered in more detail in section V. Fortunately, interstellar reddening dominates the effects of photometric errors here, and the general trend of the data in the figure does appear to suggest a normal value of R near 3. A much stronger case for a normal value of R in this region can be made using the data for stars near U Carinae (see Section VI), but there are at least no distinct features in Figure 14 which indicate any compelling need to invoke an abnormal value of R in this field. Moreover, even an abnormally large value for this region would not effect our conclusions regarding GT Car. It appears quite certain that this Cepheid is more distant than any of the B stars in its vicinity that were included in our survey.

V The Field of Trumpler 17

(a). Photometry and Field Reddening

The open cluster Trumpler 17 lies some 30' northwest of GT Car at RA 10^h 54'.2, dec $-58°$ 57' (1950.0) and falls well within the field of our photographic plates. Previous photometric investigations of this cluster include the UBV study by Sher (1964) and a more recent study using RGU photometry carried out by Steppe (1977). Of the 49 stars originally measured by Sher, only 23 were sufficiently free from crowding on plate #CF2108 to be confidently measured. Stars 57 and 59 were incorporated in the study that follows adopting the adjusted photoelectric data in Table IV. An additional 19 stars were obtained by transforming the photometry of Sher to that of this study using the stars listed in Table VIII and the following relations derived between the present photometry and that of Sher:

$$(V)danks = 0.986(V)sher[\pm0.010] + 0.22[\pm0.12] \qquad (11)$$

$$(B-V)danks = 1.21(B-V)sher[\pm0.152] - 0.089[\pm0.08] \qquad (12)$$

$$(U-B)danks = 0.704(U-B)sher[\pm0.095] - 0.016[\pm0.02] \quad (13)$$

where the '[]' symbols enclose errors in slope and intercept. Equations (11) through (13) have standard deviations

Table VIII

Stars used to transform the photometry of
Sher(1964) to that of this study

Star*	(Danks)			(Sher)		
	V	B-V	U-B	V	B-V	U-B
4	12.46	0.41	-0.28	12.40	0.42	-0.26
5	11.28	0.47	-0.15	12.20	0.52	-0.18
11	13.81	0.50	0.06	13.81	0.50	-0.02
13	11.82	0.47	-0.14	11.83	0.41	-0.19
14	11.81	0.40	-0.14	11.78	0.40	-0.24
16	12.25	0.39	-0.05	12.18	0.42	-0.11
19	11.63	0.48	-0.40	11.58	0.52	-0.50
27	11.86	0.43	-0.16	11.77	0.44	-0.06
30	13.30	0.55	-0.04	13.27	0.52	0.10
34	12.26	0.57	-0.15	12.26	0.50	-0.16
37	12.80	0.53	-0.07	12.75	0.51	-0.14
38	12.68	0.42	-0.02	12.68	0.48	-0.05
41	13.41	0.50	0.08	13.31	0.58	0.02
43	14.23	0.85	-0.01	14.23	0.79	0.12
44	13.42	0.65	0.05	13.42	0.54	0.04
47	12.57	0.56	-0.14	12.50	0.53	-0.21
48	13.56	0.62	-0.03	13.49	0.53	-0.04
49	13.77	0.74	-0.09	13.76	0.61	-0.11
58	13.56	0.63	-0.06	13.49	0.57	-0.06

* The numbering of Sher (1964) is retained

of ±0.035 mag in V, ±0.056 mag in B-V and ±0.057 mag in U-B,
respectively, for the stars in Table VIII. The stars of
Trumpler 17 are identified on the V band finder chart given
in Figure 3. The numbering system of Sher is retained. All
stars listed by Sher are labelled, but numbers 2, 15, 31,
53 and 56 were too red to be confidently transformed using
equations (11) through (13). These stars are therefore not

included in the discussion which follows. Transformed

V magnitudes and colours for those stars included in the

analysis are listed in Table IX. CC and CM diagrams for

Trumpler 17 are given in Figures 15 and 16 respectively.

Table IX

Stars in Field of Trumpler 17

Star	V	B-V	U-B
1	14.56	1.03	0.24
3	13.39	0.59	0.26
4	12.46	0.41	-0.28
5	11.28	0.47	-0.15
6	13.91	0.63	-0.02
7	10.37	0.41	-0.04
8	13.62	0.51	0.10
9	13.45	0.55	0.13
10	14.34	0.76	0.03
11	13.81	0.50	0.06
13	11.82	0.47	-0.14
14	11.81	0.40	-0.14
16	12.25	0.39	-0.05
17	13.31	0.75	0.13
19	11.63	0.48	-0.40
21	13.53	1.16	0.41
22	14.50	1.01	0.32
23	14.26	0.89	0.14
24	14.37	0.56	0.10
27	11.86	0.43	-0.16
28	14.08	0.89	0.41
30	13.30	0.55	-0.04
32	13.20	0.65	0.17
33	14.32	0.83	0.31
34	12.26	0.57	-0.15

Table IX continued

Star	V	B-V	U-B
37	12.80	0.53	-0.07
38	12.68	0.42	-0.02
39	14.12	0.77	0.13
40	14.14	0.60	0.11
41	13.41	0.50	0.08
43	14.23	0.85	-0.01
44	13.42	0.65	0.05
45	11.69	1.21	0.47
46	12.86	0.42	-0.05
47	12.57	0.56	-0.14
49	13.77	0.74	-0.09
52	14.32	0.90	0.11
54	14.52	0.57	0.15
55	14.41	0.75	0.13
57	11.48	1.04	0.79
58	13.56	0.63	-0.06
59	9.80	0.06	-0.04
60	11.64	0.33	-0.20

In this section we shall determine both the distance to and the age of Trumpler 17. To do so it will be necessary to cull field stars from Table IX, Figure 15 and Figure 16. Several factors need be considered prior to accepting or rejecting a given star as a cluster member. Among these are the interrelations of colour excess, distance modulus and spatial location as well as the position of a star with respect to the ZAMS relation in an intrinsic CM diagram. Thus, to be considered a cluster member it is desirable that:
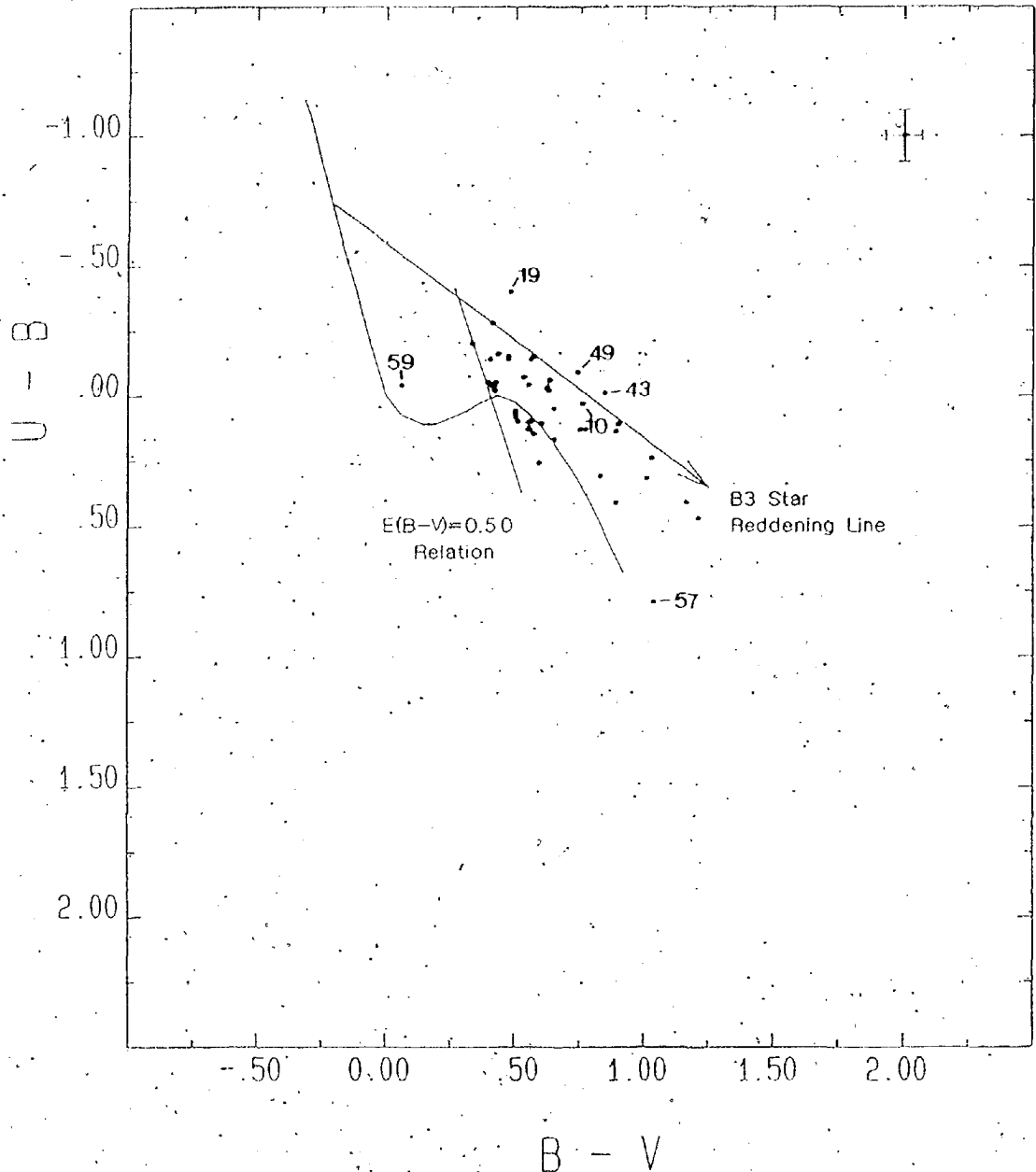
Figure 1 5

CC Diagram for Trumpler 17 Field

Error bars depicted are for one standard
deviation as explained in the text. ZAMS
relation is from Johnson (1 966). A B3 star
reddening line of slope 0.75 and a minimum
reddening relation for B dwarf cluster mem-
bers of E(B–V)=0.50 are shown. Identified
stars are discussed in the text.
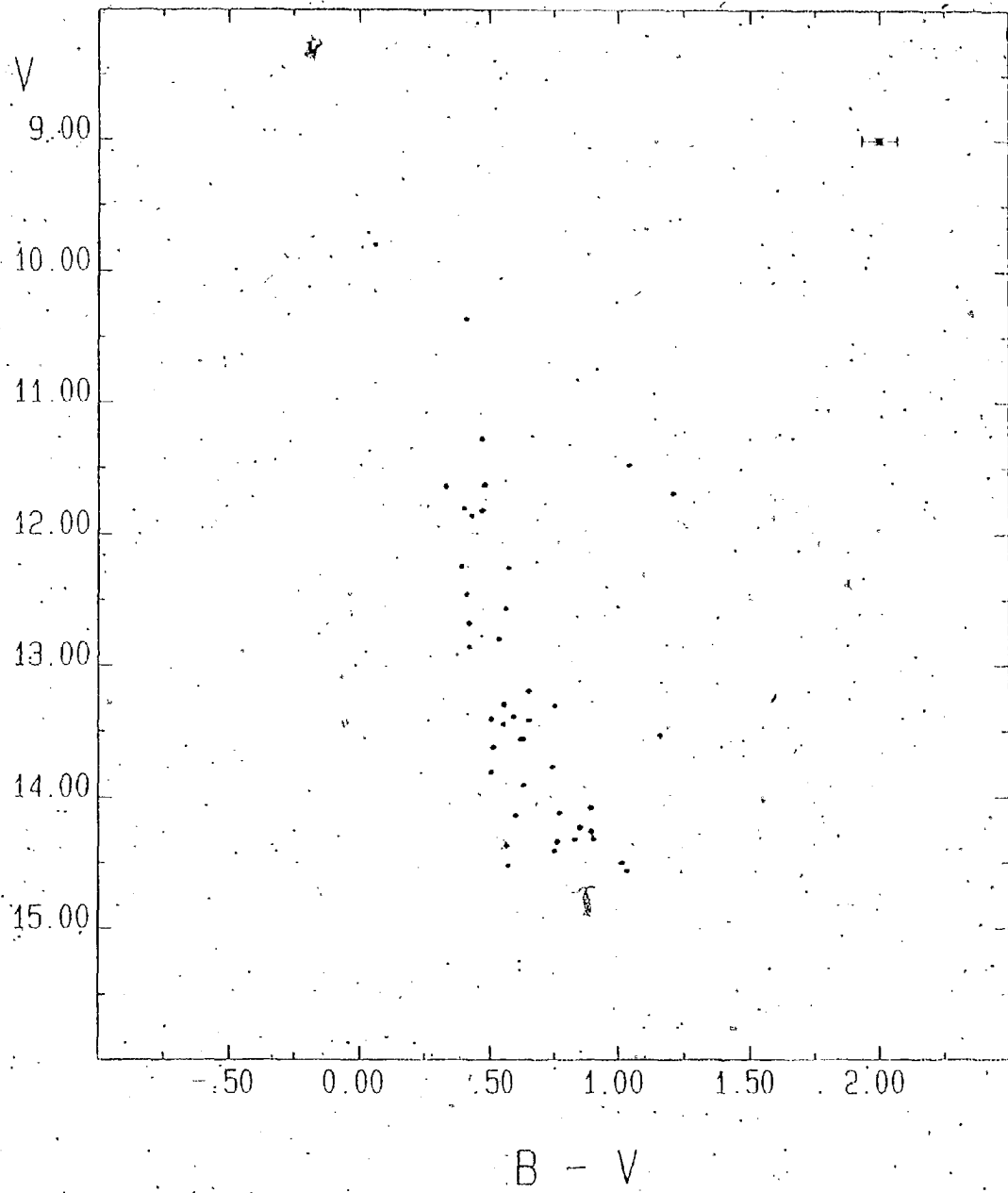
Figure 16

CM Diagram for Trumpler 17 Field

Error bars depicted are for one
standard deviation as explained in
the text.

1. A star's colour excess not be discordant with immediately adjacent cluster stars.

2. The position of the star in the V-Mv versus E(B-V) plane should be consistent with other cluster members. This requires an appreciation of the effects of systematic errors in variable extinction analysis which will be discussed presently.

3. A star lie near the line fit to the cluster sequence in an intrinsic CM diagram. Stars lying appreciably blueward of the ZAMS relation fit to unevolved cluster stars, for example, are unlikely to be members.

In the discussions to follow we shall therefore refer to the field reddening and variable extinction charts as aids in determining the group membership question as well as the CC and intrinsic CM diagrams.

An obvious feature of Trumpler 17, which will become evident in the variable extinction plot and field reddening chart, is the existence of differential reddening across the face of the cluster. This characteristic suggests use of the CC diagram in determining membership as follows. A reddening line of slope 0.75 was fit to the upper envelope of cluster stars in Figure 15. This reddening line crosses the intrinsic relation at the

colours of a B3 star, which presumably represents the blue
limit for the cluster turnoff point. A minimum reddening
relation for Trumpler 17 B dwarfs of E(B-V)=0.50 is also
depicted, and can be interpreted as the minimum foreground
reddening to the cluster. Stars located outside of the red-
dening 'wedge' formed by the intersection of these two
lines are likely field stars in that they exhibit colour
excesses or intrinsic colours incompatible with the bulk
of cluster stars. We will return to consider the case of
these and other stars individually identified in Figure
15 during discussion of the variable extinction analysis
or with reference to the intrinsic CM diagram.

All stars in Table IX were used to construct a
variable extinction plot for the field of Trumpler 17.
This appears in Figure 17 with the data tabulated in
Table X. The colour excesses given in the table were
adjusted to an equivalent B0 star reddening using
equations (9) and (10). Prior to discussing Figure 17
it is appropriate to first treat the question of sys-
tematic errors in the variable extinction technique.

(b) Errors in Variable Extinction Analysis
An attempt to fit a single line to all the stars
of Figure 17 results in a value of R near 8, an implausibly
high value for the ratio of total to selective extinction,

Table X

Distance Moduli, Colour Excesses and Intrinsic
Colours for the Stars of Trumpler 17

Star	V - Mv	Vo	(B-V)o	(U-B)o	E(B-V)
1	15.21	10.72	-0.19	-0.76	1.24
3	12.44	11.28	-0.07	-0.24	0.68
4:	13.46	10.51	-0.21	-0.75	0.63
5	11.76	9.23	-0.18	-0.63	0.66
6:	14.23	11.40	-0.17	-0.61	0.81
7	10.14	8.67	-0.13	-0.44	0.55
8	13.13	11.67	-0.11	-0.36	0.63
9	12.84	11.40	-0.10	-0.34	0.66
10	14.99	11.36	-0.19	-0.68	0.96
11:	13.45	11.86	-0.12	-0.40	0.63
13	12.14	9.77	-0.17	-0.61	0.65
14	11.98	10.04	-0.16	-0.55	0.57
16	11.89	10.64	-0.12	-0.43	0.52
17	13.21	10.49	-0.15	-0.53	0.91
19	13.53	9.34	-0.26	-0.95	0.74
21	13.56	9.41	-0.15	-0.54	1.33
22	14.53	10.84	-0.15	-0.53	1.18
23:	14.91	10.85	-0.18	-0.66	1.10
24	12.29	12.26	-0.12	-0.41	0.68
27	12.18	9.97	-0.17	-0.60	0.61
28	13.35	11.08	-0.09	-0.32	1.00
30:	13.47	11.07	-0.16	-0.56	0.72
32	12.84	10.77	-0.12	-0.41	0.79
33	13.83	11.35	-0.11	-0.40	0.96
34	13.09	9.84	-0.20	-0.73	0.78
37	12.97	10.63	-0.16	-0.57	0.70
38	12.32	10.98	-0.12	-0.43	0.55
39	14.15	10.93	-0.15	-0.54	1.02
40:	13.91	11.85	-0.13	-0.43	0.74
41	12.92	11.49	-0.11	-0.37	0.62
43	15.58	10.88	-0.23	-0.82	1.08
44	13.45	10.91	-0.15	-0.51	0.81
45	14.75	7.41	-0.15	-0.52	1.38
46	12.63	11.12	-0.13	-0.46	0.56
47:	13.40	10.18	-0.20	-0.71	0.77

Table X 'continued

Star	V − Mv	Vo	(B−V)o	(U−B)o	E(B−V)
48	13.88	11.08	−0.17	−0.61	0.80
49	15.12	10.73	−0.23	−0.81	0.98
52:	15.15	10.88	−0.20	−0.71	1.11
54:	13.91	12.41	−0.10	−0.35	0.68
55:	14.44	11.56	−0.15	−0.53	0.92
57	9.44	8.44	0.10	0.10	0.98
58:	14.21	10.99	−0.19	−0.68	0.83
59	8.55	9.49	−0.04	−0.11	0.10
60	11.81	10.12	−0.16	−0.55	0.50

: Denotes stars used to determine the distance
of Trumpler 17. See text for a discussion.

Excesses given are adjusted to an equivalent
B0 star reddening using equations (9) and (10).

even for the Carina Nebula region. In any variable extinc-
tion analysis based on photometric data there are several
processes which act to drive stars from the relation defined
by the intrinsic value of R indicated by equation (6).
Among these are the effects of random scatter in the CC
plane caused by photometric errors. Such errors translate
into systematic scatter in the variable extinction diagram,
producing artificially large values of R (Turner 1976).
This systematic effect results from the technique of using
a reddening line in the CC plane to deredden stars. The
technique leads to a direct correlation between the derived

Figure 17

Variable Extinction Plot for Trumpler 17 Field

A line of slope R=3.1 is shown at Vo–Mv=11.5 4
fitted to 11 stars in the range 13<[V–Mv]<1 5.
A line is also shown representing the Car OB1
Complex at Vo–Mv=12.07. The dashed line at
Vo–Mv=13.40 represents a background association
as in Figure 14. See text for details. Error
bars are for ±0.39 mag in V–Mv and ±0.02 mag
in E(B–V).
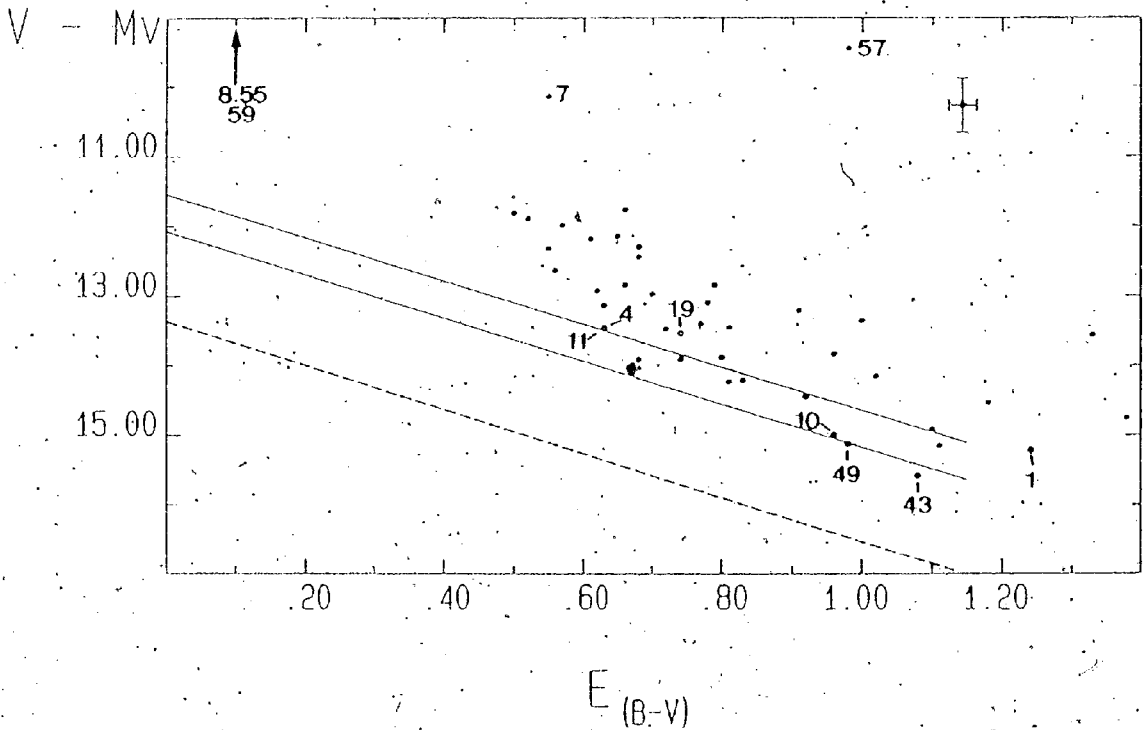
values of Mv (and hence V-Mv) and E(B-V) in the sense that
an underestimate of one due to scatter leads to an underestimate in the other. Conversely, an overestimate of E(B-V)
leads to an overestimate in V-Mv. Random scatter in UBV
photometry therefore acts to drive stars towards either
the upper left or the lower right hand corner of the
(V-Mv)-E(B-V) plane, leading to values of R that are systematically too high. In addition to photometric errors,
the accidental inclusion of foreground and/or background
field stars in the analysis will also skew the results
toward erroneously high values of R.

It was assumed during the dereddening process that
all stars were ZAMS objects. Values of Mv thus obtained
from (B-V)o-Mv(ZAMS) relations are actually upper limits
in that the luminosities derived for evolved objects
are insufficiently luminous. Indicated colour excesses
of such objects will, in addition, tend to be somewhat overestimated as well. Thus, the plotted positions of non-main
rsequence stars in the variable extinction diagram will be
shifted towards lower values of V-Mv and (slightly) higher
values of E(B-V).

The inadvertent inclusion of binary stars in the
analysis produces a similar shift toward lower values
of V-Mv as a consequence of these objects' apparent magnitudes being more luminous than those of single stars.

In appreciation of these systematic errors towards
smaller values in V-Mv, we determine distances in the
variable extinction diagram by fitting a line of approp-
riate slope to the mean position of stars lying within an
error bar of the bottom envelope of group members.

·(c)·Distance to Trumpler 17

In Figure 17, in addition to 3 stars of V-Mv<10.5,
we observe a clustering about V-Mv~12.5 and E(B-V)~0.60.
These objects are judged to lie above the line defining
the intrinsic value of R for the reasons discussed prev-
iously. Star number 59, of E(B-V)=0.10, is obviously a
foreground field star as is clearly evident from its
position in Figure 15. Star 7 is an evolved object
as is apparent from its location in the intrinsic CM
plane presented in Figure 19. Most of the stars included
in the clustering about V-Mv~12.5 and E(B-V)~0.60 are also
evolved cluster members. Multiple reddening solutions for
star number 57 (Figure 15) indicate this object to be
either a slightly reddened foreground K dwarf or an A star
of E(B-V)=0.98. We adopt the latter solution here based
upon the resulting colour excess being similar to that
of nearby star number 58 in the field reddening chart
given in Figure 18. Star 57 is plotted accordingly in
Figures 17 and 19, but a question mark is placed beside

its position in the intrinsic CM plane to emphasize the
uncertainty as to the spectral type of this object.

The two objects of largest V-Mv and correspondingly
large reddenings in Figure 17, stars 43 and 49, are
found in immediate proximity to a band of obscuring
matter skirting the northeastern boundary of the clus-
ter as analysed on the field reddening chart given in
Figure 18. This area of higher obscuration is evident
as a dust cloud on the ESO IIIa-J plate. While it is
possible that these stars suffer heavy reddening as a
result and represent a localised area with R>3.1, it
is important to note that they also lie above the B3
star reddening line in Figure 15. Since it would be
an unlikely coincidence for two of the youngest cluster
stars to lie outside the cluster proper in a pocket
of anomalous extinction, it is concluded that stars 43
and 49 are more likely to be background stars with res-
pect to Trumpler 17. Star 10 is also a likely background
star, for similar reasons. A line of slope R=3.1 is
shown in Figure 17 at Vo-Mv=12.07 representing the distance
of the Car OB1 complex. Stars 10, 43 and 49 fit the rela-
tion well, indicating that Car OB1 extends into the field
of Trumpler 17. It should be noted that the location of all
three stars in the intrinsic CM plane blueward of the stan-
dard sequence fitted to the cluster (Figure 19), gives

added weight to the interpretation of their being non-members.

To determine the distance to Tr 17 a line of slope R=3.1 was fit to the objects lying within a single error bar of the bottom envelope of stars with V-Mv>13. Stars 10, 43 and 49 were excluded for the reasons just discussed. Star 1 was excluded on the basis of its colour excess (1.24) being markedly different from the reddenings of its immediate neighbours. This star is both faint and red (V=14.56, B-V=1.03), suggesting the possibility of photometric error. Star 19 was also excluded as a cluster member from consideration of its anomalous position in both Figure 15 and the intrinsic CM plane. The 11 stars selected for determining the distance to Trumpler 17 (note that stars 4 and 11 appear superimposed in Figure 17) are designated by colons in Table X. A line of slope R=3.1 is drawn through the mean position of these 11 stars, yielding Vo-Mv=11.54 ±0.39 mag. Trumpler 17 therefore lies at a distance of 2.0 ±0.4 kpc, a value in better agreement with the 2.2 kpc found by Steppe (1977) than with the 1.4 kpc indicated by the earlier work of Sher (1964).

A space reddening chart for the field of Trumpler 17 is given in Figure 18. In contouring this chart reference was made to the ESO IIIa-J plate to supplement the E(B-V) data. The area of high extinction to the northeast of the
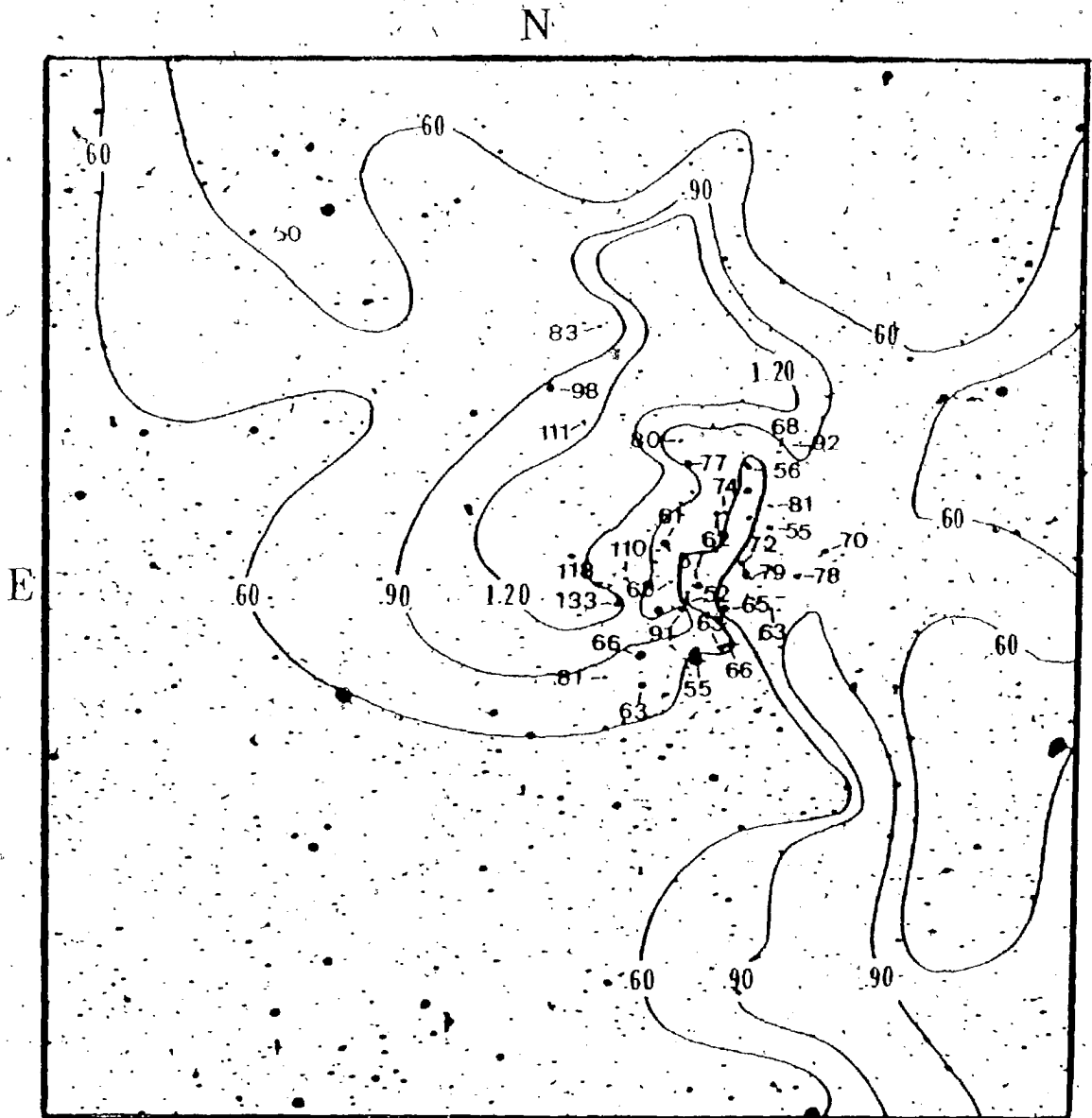
Figure 18

Field Reddening Chart for Trumpler 17

The colour excesses of Trumpler 17 members in Table
X are plotted. The field is contoured with respect
to the excesses shown and modelled to areas of obvious
field obscuration on the ESO IIIa–J plate. The
area of high extinction on the northeast shoulder
of the cluster is evident as a dust cloud on the ESO
survey. The central region of the cluster appears
to be relatively dust free. See the text for a brief
discussion.

cluster core is clearly evident as an opaque dust cloud on the ESO survey and manifests itself as a pronounced deficit of stars in this portion of the figure. The colour excesses plotted seem to indicate the cluster centre to be relatively dust free when compared to the surrounding field. This may be a chance effect produced by the shape of a foreground dust cloud. However, it may also indicate the existence of a cavity in a circumcluster dust cloud excavated by radiation pressure and/or stellar winds from cluster members. Investigations of NGC 581, 6834 and 7380 by Moffat (1971, 1972). imply the existence of similar central cavities in the space reddenings of these other young clusters.

(d) Age of Trumpler 17

All stars in Table IX were used to construct the intrinsic CM diagram for Trumpler 17 shown in Figure 19. Values of Vo, (B-V)o and (U-B)o are included in Table X. The scale ratio of Vo:(B-V)o has been expanded to 10:1 to assist in fitting the main-sequence and locating the colour of the turnoff point: The standard sequence is depicted at Vo-Mv=11.54, as derived from the variable extinction analysis discussed previously.

Considerable scatter about the standard sequence is evident. Since we are using photographic data at a large (B-V)o scale expansion, it is not unreasonable to assume
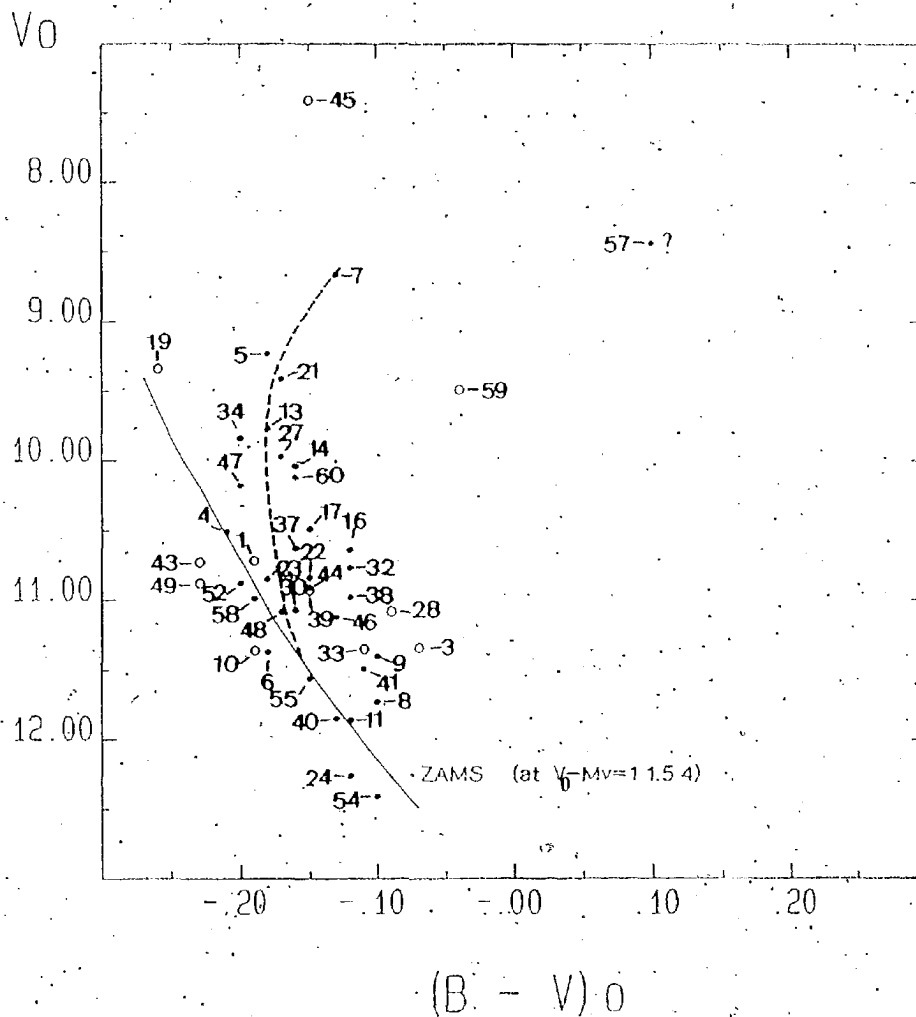
Figure 19

Intrinsic CM Diagram for Trumpler 17

The ZAMS of Turner (1976) is shown for Vo−Mv=11.54
as determined by a variable extinction analysis. Stars
determined to be non−members of the cluster are plotted
as open circles. The interrogation mark near star #57
indicates the uncertainty of the SpT for this star as
discussed in the text.

The Trumpler 17 sequence shown as a dashed line is
fitted by hand. The bluest colour reached by the cluster
sequence is estimated to be −0.18 ±0.01 mag. in (B−V)o.
The age of Trumpler 17 is discussed in the text.

that most of this scatter can be attributed to random errors in the photographic photometry. We have already noted several stars in Table IX that are unlikely to be members of Trumpler 17. In Figure 19 these probable field stars are plotted as open circles. In addition to objects already discussed, stars 28, 33, 39 and 45 are shown as non-members since their reddenings are markedly different from those of closely adjacent stars. Star 3, lying well to the red of the standard sequence, is also plotted as a non-member.

The scatter in Figure 19 makes it difficult to fit the standard sequence with confidence, but the shift of 11.54 mag suggested by our variable extinction analysis seems quite satisfactory. This is taken as corroboration for the distance derived here for Trumpler 17; i.e. 2.0 ±0.4kpc.

We show in Figure 19 a handfit to the cluster main-sequence, and estimate the bluest colour reached to be $(B-V)_0 = -0.18 \pm 0.01$ mag (a spectral type equivalent of about B4). Using the theoretical isochrones of Maeder and Mermilliod (1981), we estimate the age of Trumpler 17 to be $50 \pm 11 \times 10^6$ years. An unpublished relation of Turner, which is also based on theoretical models, yields a comparable age of 52×10^6 years for a main-sequence turnoff of $(B-V)_0 = -0.18$. This relation is quoted for reference purposes below:

$$\log t \text{ (in } 10^6 \text{ y)} = 9.19 + 8.20(B-V)o \qquad (14)$$

An age of 50 million years is considerably in excess of
the ages estimated for any known association of OB stars,
or any long-period Cepheid. We therefore suggest that Trum-
pler 17 is a sparse cluster which is both older than and
foreground to the stars in its vicinity which belong to
the Car OB1 association.

VI   The Field of U Carinae

(a) Preliminary Remarks

The bright, long-period [$<V>=6.273$, $P=38.7614d$] Cepheid U Carinae [RA 10^h 55^m 46^s dec $-59°27'.8$ 1950] falls well within the field of our photographic plates [Figure 3a, p17]. This is one of the longest period Cepheids in the Galaxy and is therefore, of particular value in the calibration of the high luminosity end of the P-L relation. Furthermore, its brightness suggested a much better possibility of detecting associated stars with our plate material than was the case for GT Car. Therefore, the field of U Car was examined and analysed using similar techniques as were applied to the fields of Trumpler 17 and GT Car. In addition, data for stars lying within 2 degrees of U Car were selected from southern OB star catalogues and analysed using the variable extinction method to detect likely associates of the Cepheid.

(b) Field Reddening

To complement the variable extinction plot and space reddening chart of the U Car field, we have made use of the photometry published in van den Bergh et al.

(1984). To maintain consistency with the photometry of this study, that of van den Bergh et al. was transformed using the early-type stars listed in Table XI, which were measured on our plates, and the following relations derived from a least squares fit:

$$(V)danks = 0.942(V)vdb[\pm0.024] + 0.72[\pm0.31] \qquad (15)$$

$$(B-V)danks = 0.859(B-V)vdb[\pm0.146] + 0.06[\pm0.30] \qquad (16)$$

$$(U-B)danks = 0.739(U-B)vdb[\pm0.088] - 0.07[\pm0.02] \qquad (17)$$

where the '[]' symbols enclose error values for slope and intercept. Equations (15) through (17) have standard deviations of ±0.034 mag in V, ±0.029 in B-V and ±0.023 in U-B for the stars of Table XI.

Table XI

Stars Used to Transform the Photometry of van den Bergh et al. (1984) to that of this study

Star*	(Danks) V	B-V	U-B	(vdB) V	B-V	U-B
37	12.88	0.20	-0.14	12.90	0.15	-0.06
44	12.16	0.14	-0.35	12.18	0.09	-0.38
135	12.71	0.10	-0.16	12.75	0.11	-0.12
154	13.15	0.28	-0.18	13.17	0.28	-0.15
230	13.76	0.24	-0.16	13.92	0.16	-0.17
288	13.48	0.22	-0.33	13.57	0.16	-0.31
294	13.78	0.27	-0.18	13.83	0.25	-0.14
322	13.15	0.33	-0.20	13.20	0.31	-0.21

Data for the stars in the U Car field, including

the stars measured for this study as well as values obtained by transforming the photometry of van den Bergh et al., are listed in Table XII. The tabulated colour excesses were adjusted to an equivalent B0 star reddening using equations (9) and (10). Stars were dereddened to the intrinsic relation of Johnson (1966). A reddening line of slope $E(U-B)/E(B-V)=0.75$ was used, as adopted for the GT Carinae field. The corresponding variable extinction plot is given in Figure 20. Error bars shown probably do not reflect the true uncertainty associated with more distant objects due to a lack of suitably faint stars used to derive the transformation relations given in equations (15) to (17). However, as only stars lying less distant than the Car OB1 association were used in deriving a reddening for the U Car field, this objection is not considered serious.

To determine the position of U Car in Figure 20 we used the values $<V>=6.273$ and $P=38.7614d$ for this star tabulated by Schaltenbrand and Tammann (1971). The period-luminosity relation of van den Bergh (eqn. 7) yields $Mv=-5.79\pm0.26$ for a Cepheid of this period. Fernie and Hube (1968) quote -5.93 for the absolute magnitude of this star, as computed from Fernie's period-luminosity relation. A mean of these values for $M<v>$ is adopted here. We thus calculate $<V>-M<v>=12.13$ for U Car.

Table XII

Data for Stars in The U Carinae Field

Star	V	B-V	U-B	(B-V)o	V-Mv	E(B-V)
1:	14.27	0.66	0.20	0.39	10.81	0.29
2	14.84	0.82	-0.03	-0.22	16.01	1.05
4	15.27	0.66	-0.01	-0.17	15.59	0.84
5	14.33	0.49	-0.03	-0.14	14.23	0.64
6	15.26	0.76	0.08	-0.17	15.58	0.94
8:	13.42	0.75	0.21	0.44	9.60	0.33
9	15.14	0.69	-0.11	0.22	16.31	0.92
10:	14.91	0.85	0.15	-0.17	15.23	1.04
11	15.13	0.48	0.06	-0.11	14.64	0.60
14	14.40	0.57	-0.03	-0.16	14.57	0.74
15	15.05	0.84	0.14	-0.17	15.37	1.03
16	14.56	0.89	0.02	-0.24	16.08	1.14
17:	13.58	0.36	0.16	-0.05	12.43	0.42
18	14.73	0.39	-0.12	-0.15	14.76	0.55
19	14.72	0.24	0.07	-0.04	14.62	0.29
22	13.79	0.45	-0.11	-0.20	14.62	0.66
23	14.14	0.58	-0.03	-0.14	13.31	0.75
24:	12.35	0.26	0.03	-0.07	11.40	0.34
25	13.82	0.49	-0.10	-0.19	14.47	0.69
26:	13.47	0.54	0.00	-0.14	13.37	0.68
27	14.27	0.30	0.03	-0.07	13.32	0.38
29:	13.48	0.31	0.18	-0.02	12.06	0.34
31:	14.57	0.66	-0.05	-0.19	13.84	0.85
32:	12.92	0.41	0.16	-0.06	11.86	0.48
33	14.38	0.33	0.08	-0.07	13.43	0.40
34	15.35	0.34	0.01	-0.09	14.62	0.44
35	14.85	0.38	-0.12	-0.14	14.75	0.53
36	14.55	0.40	-0.13	-0.16	13.98	0.57
37:	12.88	0.20	-0.14	-0.11	12.39	0.32
38	15.49	0.51	-0.16	-0.18	15.97	0.70
39	15.37	0.17	0.09	-0.02	13.95	0.20
40:	13.29	0.52	-0.04	-0.15	13.32	0.68
41:	13.88	0.55	0.09	-0.18	14.36	0.74
42	14.93	0.47	0.13	-0.08	14.08	0.56
43	15.59	0.54	-0.09	-0.17	15.91	0.72

Table XII continued

Star	V	B-V	U-B	(B-V)o	V-Mv	E(B-V)
44:	12.16	0.14	-0.35	-0.18	12.64	0.32
45	14.70	0.76	-0.11	-0.24	16.22	1.01
46	15.35	0.24	-0.11	-0.11	14.86	0.36
49:	13.14	0.34	0.19	-0.02	11.72	0.37
50:	13.14	0.30	0.14	-0.03	11.80	0.34
51	15.11	0.61	-0.01	-0.16	15.28	0.78
52:	15.07	0.76	0.36	0.33	11.99	0.46
54	14.30	0.56	-0.42	-0.29	17.00	0.85
56:	13.96	0.72	0.31	0.35	10.77	0.39
57	14.66	0.64	-0.11	-0.21	15.66	0.86
58	14.56	0.69	-0.08	-0.21	15.56	0.91
59	14.10	0.65	-0.11	-0.21	15.10	0.87
61	15.16	0.61	-0.08	-0.19	15.81	0.81
64:	14.01	0.59	-0.04	-0.17	14.33	0.77
65:	13.08	0.58	-0.08	-0.18	13.56	0.77
66:	14.35	0.59	-0.15	-0.11	13.86	0.71
67:	12.75	0.44	0.00	-0.11	12.26	0.56
68:	13.96	0.60	0.00	-0.16	14.13	0.77
69:	12.01	0.70	0.26	-0.10	11.40	0.82
70	14.58	0.58	-0.01	-0.15	14.61	0.74
71:	13.59	0.62	0.00	-0.16	13.76	0.79
74:	13.96	0.45	0.14	-0.08	13.11	0.54
75	15.29	0.85	0.06	-0.20	16.12	1.06
76:	13.91	0.58	-0.04	-0.16	14.08	0.75
78	14.61	0.62	-0.01	-0.17	14.93	0.80
79:	14.12	0.46	0.11	-0.09	13.39	0.56
80	15.09	0.72	0.01	-0.18	15.57	0.91
81	14.98	0.57	-0.11	-0.19	15.63	0.77
82	15.25	0.65	-0.04	-0.19	15.90	0.85
83:	13.33	0.40	0.11	-0.08	12.48	0.49
85:	13.14	0.45	0.17	-0.07	12.19	0.53
87	14.67	0.51	0.02	-0.13	14.44	0.65
88:	11.07	0.07	-0.49	-0.20	11.90	0.27
89:	14.77	0.45	0.21	-0.05	13.62	0.51
90	14.28	0.48	-0.19	-0.20	15.11	0.69

Table XII continued

Star	V	B-V	U-B	(B-V)o	V-Mv	E(B-V)
91	14.38	0.27	-0.07	-0.12	14.02	0.40
93:	13.47	0.54	0.04	-0.13	13.24	0.68
94	14.54	0.53	-0.10	-0.18	15.02	0.72
95	14.52	0.32	0.10	-0.06	13.46	0.39
96	14.65	0.58	-0.07	-0.18	15.13	0.77
98	14.37	0.57	0.01	-0.15	14.40	0.73
99	15.09	0.68	-0.08	-0.21	16.09	0.90
100	14.31	0.33	0.09	-0.06	13.25	0.40
108	14.05	0.29	-0.02	-0.09	13.32	0.39
134:	13.16	0.11	-0.22	-0.11	12.67	0.22
135:	12.71	0.10	-0.16	-0.09	11.98	0.19
138:	13.70	0.22	0.06	-0.04	12.45	0.27
148	13.30	0.50	-0.04	-0.15	13.33	0.66
149:	14.02	0.28	0.11	-0.04	12.77	0.33
153	15.04	0.25	-0.17	-0.13	14.81	0.39
154:	13.15	0.28	-0.18	-0.14	13.05	0.43
166	15.23	0.27	-0.01	-0.08	14.17	0.36
181:	11.53	0.11	-0.08	-0.06	10.47	0.17
191	14.20	0.52	-0.25	-0.23	15.55	0.76
198:	13.72	0.51	-0.13	-0.17	14.04	0.69
225	14.03	0.41	-0.17	-0.20	14.86	0.62
228	14.12	0.30	0.06	-0.07	13.17	0.38
230	13.76	0.24	-0.16	-0.13	13.53	0.38
241	14.13	0.30	0.03	-0.08	13.28	0.39
247:	14.00	0.22	0.03	-0.06	12.94	0.29
250:	12.73	0.22	-0.06	-0.08	11.88	0.31
251	14.63	0.33	0.00	-0.09	13.90	0.43
276	14.26	0.25	-0.32	-0.18	14.74	0.44
280:	13.84	0.15	0.00	-0.04	12.59	0.20
288	13.48	0.22	-0.33	-0.20	14.31	0.43
291	14.33	0.27	0.07	-0.06	13.27	0.34
294	13.78	0.27	-0.18	-0.14	13.68	0.42
310:	11.97	0.39	-0.35	-0.24	13.49	0.64
322:	13.15	0.33	-0.20	-0.16	13.32	0.50
328:	12.36	0.21	-0.06	-0.08	11.51	0.30

Table XII continued

Star	V	B-V	U-B	(B-V)o	V-Mv	E(B-V)
336	14.41	0.29	0.04	-0.07	13.46	0.37
341	14.66	0.27	0.09	-0.05	13.51	0.33
342:	13.96	0.31	0.09	-0.06	12.90	0.38
372:	11.84	0.15	0.06	-0.02	10.42	0.17
377:	14.35	0.34	0.09	-0.07	13.40	0.42
385	14.70	0.29	0.03	-0.07	13.75	0.37
U/B:	13.03	0.63	0.18	0.39	9.57	0.26
U/C:	12.13	0.15	0.04	-0.03	10.79	0.19
U/D:	13.02	0.48	0.23	0.28	10.20	0.21
U/E:	13.91	0.52	0.06	0.42	10.23	0.11
U/F:	13.53	0.41	0.08	0.35	10.34	0.06
U/G:	15.51	0.66	0.34	0.30	12.58	0.38

: Denotes stars used to determine the field reddening in Figure 21.

Dean, Warren and Cousins (1978) have tabulated mean reddenings for Cepheids determined both by SpT-(B-V) relations and photometric two colour techniques. Their value of E(B-V)=0.28 for U Car is adopted here, but adjusted to 0.29 to conform to a zero-point shift advocated by Turner, Leonard and English (1987). Using equations (8), (9) and (10) we compute an equivalent B0 star reddening for U Car of 0.33 mag and place the Cepheid in Figure 20 accordingly.

Figure 20 shows most of the stars in the field to be at a distance comparable to or greater than that of the Car OB1 Complex at Vo-Mv=12.07 (2.6 kpc). Moreover the lower envelope trend in the data argues strongly for a

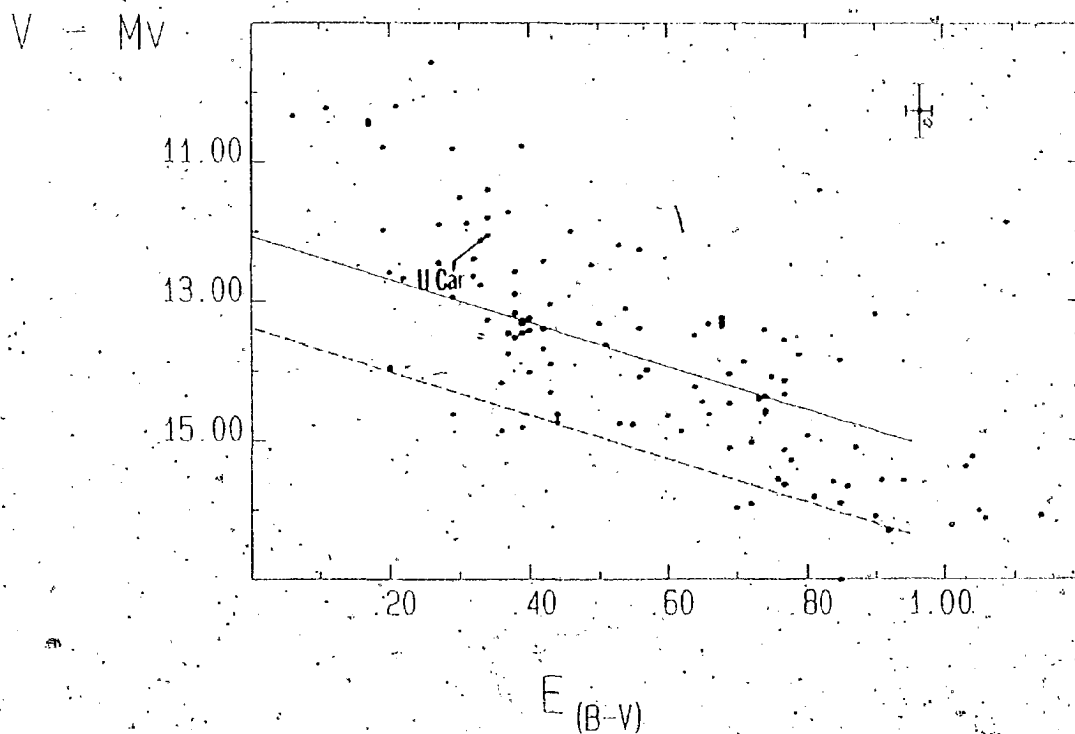Figure 20

Variable Extinction Plot for U Car Field Stars
of Table XII

A solid line of slope R=3.1 is shown at Vo−Mv=12.07,
the distance modulus of the Car OB1 Complex. Stars
less distant than this association are used to contour
the field reddening chart given in Figure 21. The
dashed line represents a background association at
Vo−Mv=13.40 as in Figures 14 and 17. Error bars cor-
respond to ±0.39 mag in V−Mv and ±0.02 mag in
E(B−V).

normal value of R~3 in this field. U Car appears to be a foreground object with respect to the Car OB1 association. The dominant dust complexes in this region appear to lie either foreground to, or in immediate association with, Car OB1 (see Neckel and Klare 1980). Therefore, to estimate the field reddening at the distance of the Cepheid the analysis was restricted to stars of Vo-Mv<12.07. These stars are flagged with colons in Table XII, and their colour excesses are shown plotted in Figure 21. We note that the stars nearest to U Car in the figure, numbers 1, 17 and 24, have E(B-V) values of 0.29, 0.42 and 0.34 respectively. These three stars bracket the Cepheid at angular separations of ~ 1 arcminute or less. A best estimate for the field reddening of U Car, based upon the colour excesses of these stars weighted according to the inverse of their distance from the Cepheid, is E(B-V)(B0) =0.34 ±0.03 s.e. or E(B-V)=0.30 ±0.03 for a star with the colours of U Car. This value agrees well with the reddening value for this star published by Dean et al. (1978).

(c) Stars Associated with U Carinae

i/ Distance

A search through the catalogues of Klare and Neckel (1977); Schild et al. (1983) and Garrison et al. (1977)
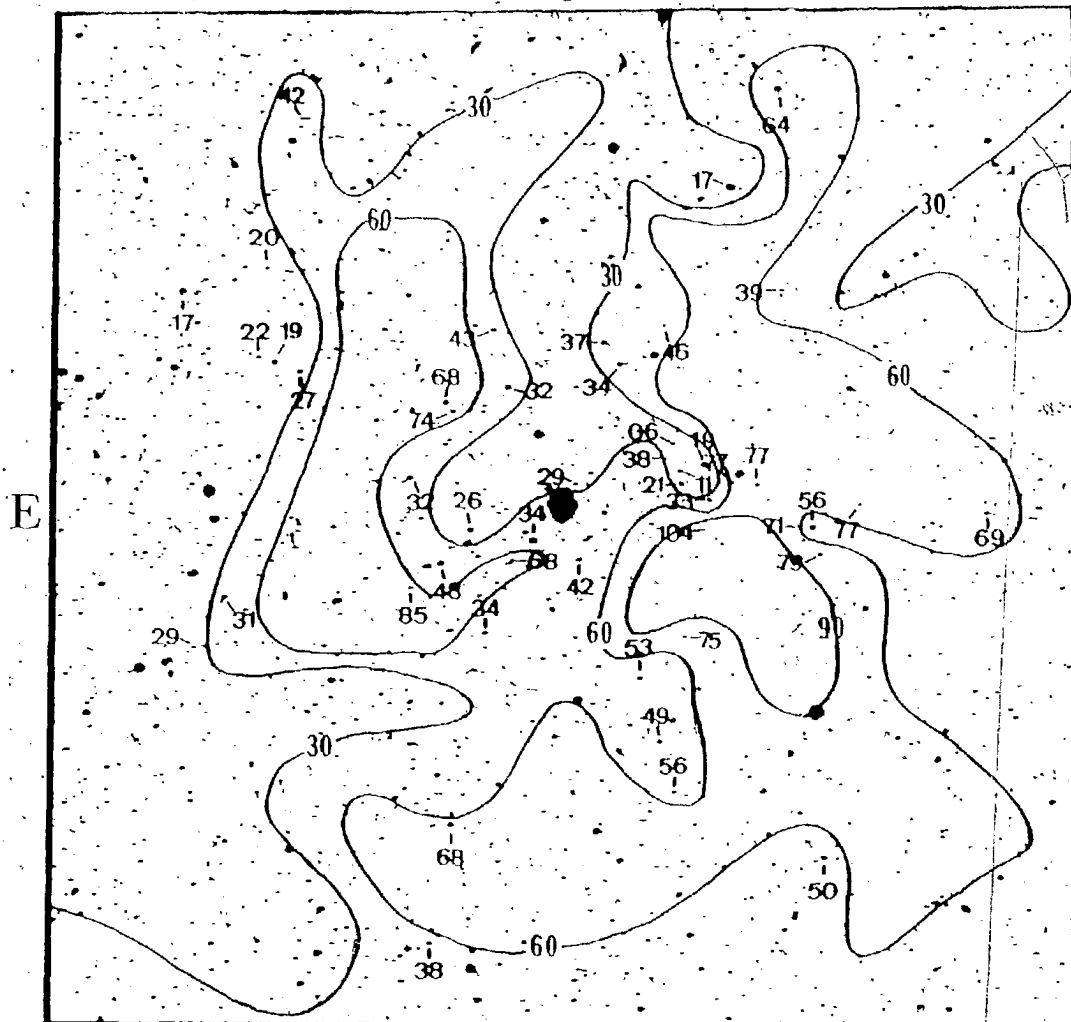
Figure 21

Field Reddening Chart for U Car

Isopleths of E(B–V) are depicted using the colour
excesses of those stars in the field lying closer
than the Car OB1 Complex as determined by the
variable extinction analysis. These stars are
flagged with colons in Table XII. Excesses have
been multiplied by 1.00 for plotting purposes.
Contours are modelled to areas of obvious field
obscuration on the ESO IIIa–J plate.

yielded 18 OB stars lying within 2 degrees of U Carinae

and having sufficiently accurate luminosities based upon

their spectral classifications to apply the variable

extinction method. These data are given in Table XIII,

where magnitudes and colours are averages from the cat-

alogues. Colour excesses were determined by comparing

these colours with the intrinsic colours predicted for

their spectral types and luminosity classes. Distance

moduli were then computed from the Mv-SpT relation of

Turner (1980) using the quoted MK spectral classific-

ations. A variable extinction plot for the stars of

Table XIII is given in Figure 22.   U Car is placed

according to the data cited previously.

A solid line of slope R=3.1 is shown in Figure 22 at

Vo-Mv=12.07 representing the Car OB1 complex. We note that

the spectroscopic data confirm the existence of the more

distant group detected in Figure 14. We determine the dis-

tance to this group by merging the photometric data for

stars 48 and 63 of Table VII with the spectral data for the

four most distant objects in Figure 22. A line (dashed

in Figures 14, 17 and 22) of slope 3.1 drawn through the

mean position of these 6 objects yields Vo-Mv=13.40

(4.8 kpc).

Four field stars which appear to share a common

distance are identified by their HD/HDE numbers in Figure

Table XIII

Catalogue Data for OB Stars within 2 degrees
of U Carinae.

r*	Star:	V	B-V	U-B	E(B-V)	V-Mv	SpT
1.39	476	9.05	0.74	-0.24	0.97	15.25	B0.7Iab
0.81	480	7.78	0.36	-0.57	0.59	13.68	B1Ib
0.99	481	10.42	0.14	-0.67	0.40	14.72	b1iii
1.51	94304	6.85	0.49	-0.27	0.57	13.35	B5Iab !
0.74	484	9.00	0.06	-0.77	0.34	13.50	B0.5III
1.23	487	7.25	0.01	-0.83	0.23	12.95	B1Ib
0.64	305771	9.62	0.19	-0.54	0.42	13.02	B2IV
0.41	500	11.40	0.17	-0.57	0.41	14.50	b2iv
0.24	502	8.89	0.04	-0.81	0.33	13.49	B0.5IVn
0.46	504	8.81	0.41	-0.55	0.65	15.31	B0.5Iab
0.82	505	9.49	0.33	-0.59	0.62	14.49	B0III
0.57	508	9.63	0.17	-0.62	0.37	14.43	B2IIn
1.11	509	9.11	0.37	-0.58	0.66	14.31	B0II-III
0.62	95880	6.96	0.32	-0.40	0.42	12.96	B5Ib !
0.76	512	9.28	0.09	-0.76	0.38	13.58	B0V
0.94	514	8.38	0.10	-0.76	0.39	13.48	B0.5III
1.19	518	7.43	0.14	-0.76	0.45	13.33	O8Ib(f)
1.87	97557	7.23	-0.01	-0.69	0.16	12.23	B2II !

Magnitudes and colours are averages from Klare
and Neckel (1977) and Schild et. al. (1983).

r*   Angular distance in degrees from U Car

:   Klare and Szeidl numbers as in Klare and Neckel
(1977) except stars found to be associated
with U Car.   These are identified by their HD/HDE
numbers.

SpT as in Garrison et al. (1977) except ! from
Humphreys (1973) and those in small script which
are MK types from Klare and Neckel (1977) as
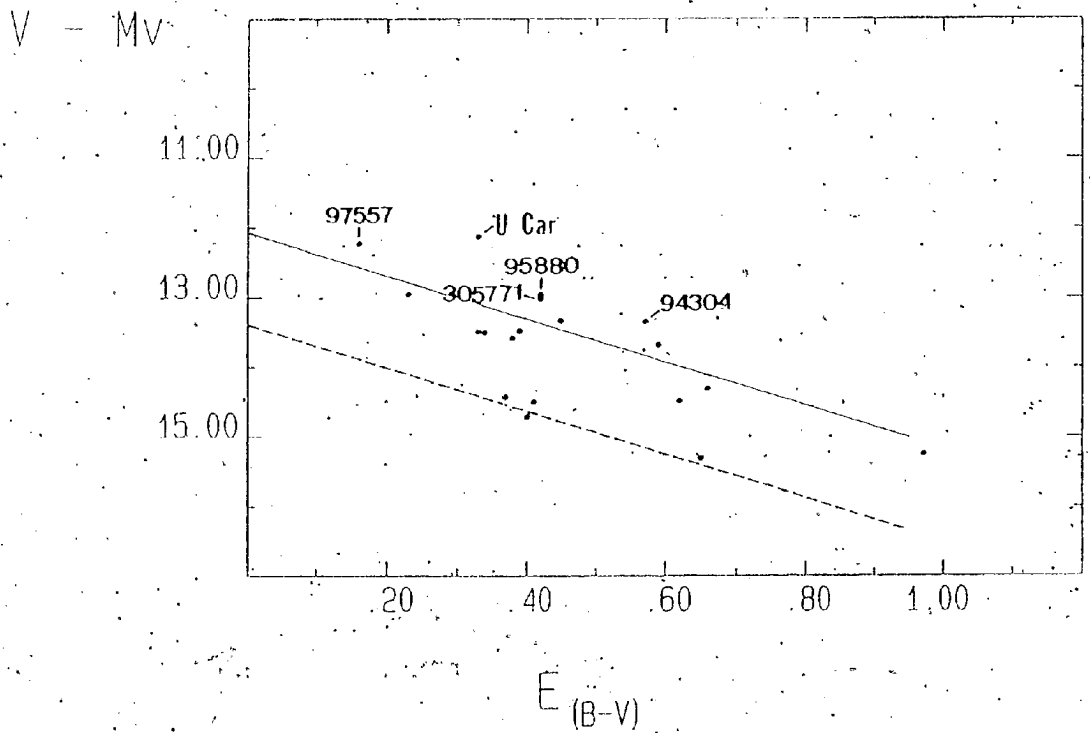inferred from photometric data.

Figure 22

Variable Extinction Plot for U Car Field Stars
of Table XIII

A solid line of slope R=3.1 is shown at Vo−Mv=12.07 cor−
responding to the distance of the Car OB1 Nebula complex.
A background association is indicated by the dashed line
at Vo−Mv=13.40. Stars identified by HD/HDE numbers are
probably associated with U Car as discussed in the text.

22, and we argue below that they are associated with U Car. The other stars in the field cluster closely to the relations representing the Car OB1 complex and the more distant group. The spectral classifications of the four nearest OB stars clearly identify them as being amongst the oldest early-type stars in the field, an important characteristic for their possible association with U Car. While the position of U Car in Figure 22 does not immediately indicate that the Cepheid is associated with any of the four selected stars, additional arguments can be presented on this question.

ii/ Radial Velocity

Available radial velocity data for U Car and 3 of the 4 stars identified in Figure 22 are given in Table XIV. The mean of the radial velocities for stars HD 94304, 95880 and 97557 is +0.2 km/s (±2.8 km/s s.e.). This value is virtually identical to the radial velocity of +0.4 km/s for U Carinae (Stibbs 1955), and is significantly different from the radial velocities (of order -20km/s) observed for the more distant OB stars in the same field (Humphreys 1973). It seems reasonable to conclude from this that U Car must be closely associated spatially with this subset of four stars.

Table XIV

Radial Velocity Data for the Stars of
Figures 22, 23 and 24

Star(HD/HDE)	Source	Vr (km/s)
94304	1	+1.4
95880	1	+4.4
97557	1	-5.2
305771	-	-
U Car	2	$<Vr> = +0.4$

1. Humphreys (1973). Weighted where
   multiple values with probable errors
   are quoted.
2. Stibbs (1955)

iii/ Age

In addition to lying at similar distances and having
similar radial velocities, the stars of Table XIV, includ-
ing U Car, also appear to be coeval. This can be demons-
trated more clearly by means of a theoretical HR diagram,
the $\log L/L_\odot - \log T_{eff}$ plane. This plane is shown in
Figure 23 on which evolutionary tracks from Maeder (1981)
are given. Maeder's case B is illustrated (i.e. cases of
intermediate mass loss) and the tracks depicted are for
$9M_\odot$ and $15M_\odot$ stars of composition X=0.70, Z=0.03, approp-
riate for young Population I stars. In order to place the
stars of Table XIV as accurately as possible in the
$\log L/L_\odot - \log T_{eff}$ plane, data (photometry, spectral clas-
sifications) from the catalogue of Humphreys (1973) were
combined with that of Table XIII. The stars were again

Figure 23

Log L/Lo--log T eff. Plane

Evolutionary tracks depicted are for a 15Mo
and a 9Mo star, after Maeder (1981). Ages
are in My. The positions of U Car and the
stars of Table XVI are shown. See the text
for a discussion.
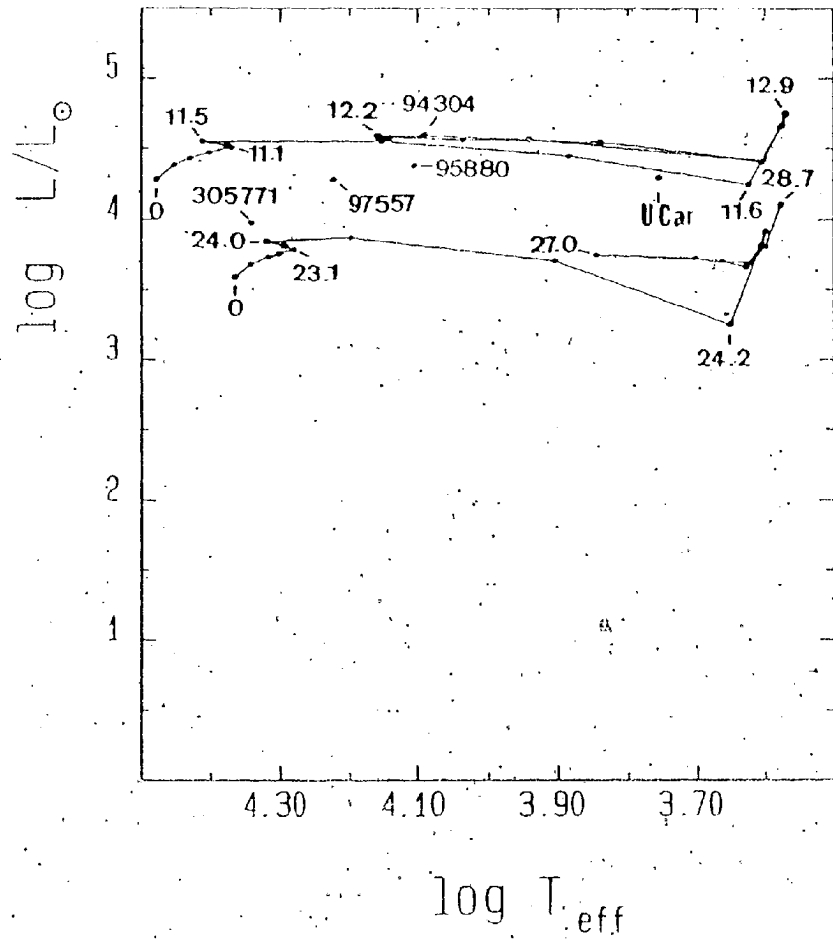
dereddened as discussed previously, and new values of
(B-V)o obtained. The resulting colour excesses were adjus-
ted to an equivalent B0 star reddening using equations (9)
and (10), and values for Vo computed assuming R=3.1. The
distance modulus for each star was determined using the
mean value of the absolute magnitudes derived from the
SpT-Mv relation of Turner (1980) and from their observed
H-beta line indices (transformed to absolute magnitudes
using the intermediary of the H gamma calibration of Mill-
ward and Walker 1985) using the photometry of Klare and
Neckel (1977). These data are given in Table XV. The
values of Vo and <Vo-Mv> in Table XV were used to cal-
culate an absolute magnitude for each star appropriate to
the group distance. This procedure ensures a set of values
for Mv that are mutually consistent, i.e., with stars
placed at a common distance. Finally, bolometric correc-
tions (Pala, 1979) were applied and log $L/L_\odot$ values for
each star computed. The data used to place the field stars
in the log $L/L_\odot$ - T_{eff} plane are given in Table XVI.

Interestingly enough, the adoption of absolute
magnitudes for the B stars based upon hydrogen beta
photometry as well as MK types has the effect of
decreasing the distance of the group to a value more
comparable with that estimated for U Car (i.e., <Vo-Mv>
=11.28 in Table XV versus Vo-Mv~11.6 for the 4 stars in

Table XV

Dereddened Data for Field B Stars Associated
with U Carinae

Numbers in parentheses refer to the sources
listed below.

Star	$<V>$ $<B-V>$(1) $<U-B>$	SpT(2)	$[B-V]o$(3)	$E(B-V)$(4)	$Vo(R=3.1)$	$Vo-Mv$(5)
94304	6.85 0.49 -0.25	B5Iab	-0.09	0.60	4.99	11.03
95880	6.94 0.32 -0.39	B5Ib	-0.10	0.44	5.58	11.52
97557	7.23 0.00 -0.67	B2II	-0.19	0.20	6.61	11.18
305771	9.62 0.19 -0.54	B2IV	-0.24	0.45	8.23	11.40
						$<11.28>$

(1) Mean values from Klare and Neckel (1977), Schild et al. (1983) and Humphreys (1973). Note that HDE 305771 does not appear in Humphreys.

(2) As in Humphreys except HDE 305771 from Garrison et al. (1977).

(3) Mean colours dereddened to standard sequences of Johnson (1966) and Fitzgerald (1970).

(4) Adjusted to equivalent B0 star reddenings using equations (9) and (10).

(5) $<Mv>$ averaged from SpT-Mv and H beta-Mv relations as explained in the text.

Table XVI

Data for log $L/L_\odot$ - log T_{eff} Plane

Numbers in parentheses refer to the sources
listed below.

Star	log T_{eff} (1)	Mv(2)	B.C. (3)	log L/L (4)
94304	4.090	-6.29	-0.49	4.60
95880	4.104	-5.70	-0.54	4.38
97557	4.224	-4.67	-1.32	4.28
305771	4.342	-3.05	-2.19	3.98
U Car	<3.755>	<-6.03>	0.00	4.30

(1) Relation of Bohm-Vitense (1981) using (B-V)o
     values of Table XV. T_{eff} for U Car from
     Parsons (1971).

(2) Computed using Vo values from Table XV and
     <Vo-Mv>=11.28 as explained in the text.

(3) Pala (1979), except that for U Car from Flower
     (1977).

(4) Assuming Mv=4.79 and B.C.=-0.07 for the Sun.

Figure 22). This is not entirely unusual since the

spectral types of these stars (B5Iab, B2II, etc.)

lie in a poorly calibrated portion of the H-R diagram,

where Mv values are often uncertain by ± 0.5 to ± 1.0

magnitudes. The hydrogen beta photometry for these stars

is particularly valuable for specifying the luminosities

with a greater degree of precision.

It may be seen from Figure 23 that, in approximate

terms, the four field stars and U Car represent an evol-

utionary sequence intermediate in mass to the $9M_\odot$ and $15M_\odot$
tracks shown. Furthermore, with the exception of HDE
305771, the stars are associated theoretically with the
rapid evolutionary phases of shell H or core He burning.
HDE 305771, the lowest luminosity star in the group, appears
to be in the last stages of MS core H burning. No attempt
is made here to offer other than very approximate ages for
these stars from consideration of their positions in the HR
diagram. An age of between 12-20 My seems appropriate
from comparison with Maeder's models.

An age estimate for U Car was obtained from the fol-
lowing relation tabulated by Tammann (1970) and making
use of old evolutionary models calculated by Kippenhahn
and Smith (1969):

$$\log t \ (\text{in } 10^6 \ y) = 1.16 - 0.651 \log P \ (d) \tag{18}$$

Using $P = 38.7614d$ (Schaltenbrand and Tammann 1971),
we compute the age of U Car to be 13My. We may consider
this to be a lower limit in that eqn. (18) makes no
allowance for core-overshooting, a physical characteristic
incorporated into current evolutionary models but not
included in the models used by Tammann. This effect
increases the core H burning MS phase of a $15M_\odot$ star by
36% (Cloutman and Whitaker 1980). We arbitrarily increase
the age of U Car computed from Tammann's relation by this
same amount to arrive at a final estimated age of 18 My.

The consistency of these estimates in conjunction with the location of these four stars in Figure 22 is a convincing argument for their coevality. U Car and these four stars almost certainly form a physical association.

VII Discussion and Conclusions

In this thesis we have been concerned with methods by which clusters or associations in proximity to long-period Population I galactic Cepheids might be detected. The detection of significant numbers of such cases would present an opportunity to verify or refine the high luminosity end of the Period-Luminosity Law by deriving distances to the stellar groups in which these stars are located. Such an opportunity is to be welcomed in that the extragalactic distance scale is sensitive to the calibration of Population I Cepheid luminosities. Previous such investigations (van den Bergh, et al., 1976, 1982, 1983, 1984) have attempted to locate Cepheids in associations by analysing only CC and CM diagrams of surrounding fields. In order for such methodology to be successful it is necessary that any cluster or association present in the field be sufficiently rich that a significant number of group members will be detected within a small angular distance of the Cepheid. If an insufficient number of members is detected, they will be swamped by field stars in the CC and CM planes and their significance overlooked. Furthermore, a major disadvantage in relying totally on CC and CM diagrams is that differential reddening, a common

feature in young clusters and particularly of associations,
acts to mask the presence of such stellar groups in these
diagrams. We have demonstrated that the variable extinction
method of analysis actually uses this phenomenon to better
the chance of detecting the presence of clusters or assoc-
iations in the field.

In van den Bergh et al. (1984) it was concluded
that no early-type stars had been detected in association
with U Car. This conclusion was based solely on the
analysis of CC and CM diagrams of several hundred stars
within 10' of the Cepheid, methodology initially emulated
in this paper for the GT Car field. In contrast, from con-
sideration of distances determined by variable extinction
analysis, radial velocity and age, it is here suggested
that 4 B type stars are likely to be physically associated
with U Car. The positions of these four stars and that of
U Car are shown in new galactic coordinates in Figure 24.
The position of Trumpler 17 is also indicated. The scale
depicted is valid at the distance determined by the mean
distance modulus of the group corrected for reddening
($<Vo-Mv>=11.28$ Table XV), i.e. 1.8 kpc. The maximum
separation of any of these objects (stars HD 94304 and
97557) is found to be 92.5 pc. Using 18My as the age of
the Cepheid we compute a velocity spread of ±2.5 km/s to
be sufficient to account for the observed separations

Figure 24

Space Position Plot

The positions of the objects in Table XV
are shown in new galactic coordinates. The
location of the young cluster Trumpler 17
is also indicated. The scale depicted is
valid at the distance of U Car, i.e. 1.8 Kpc.
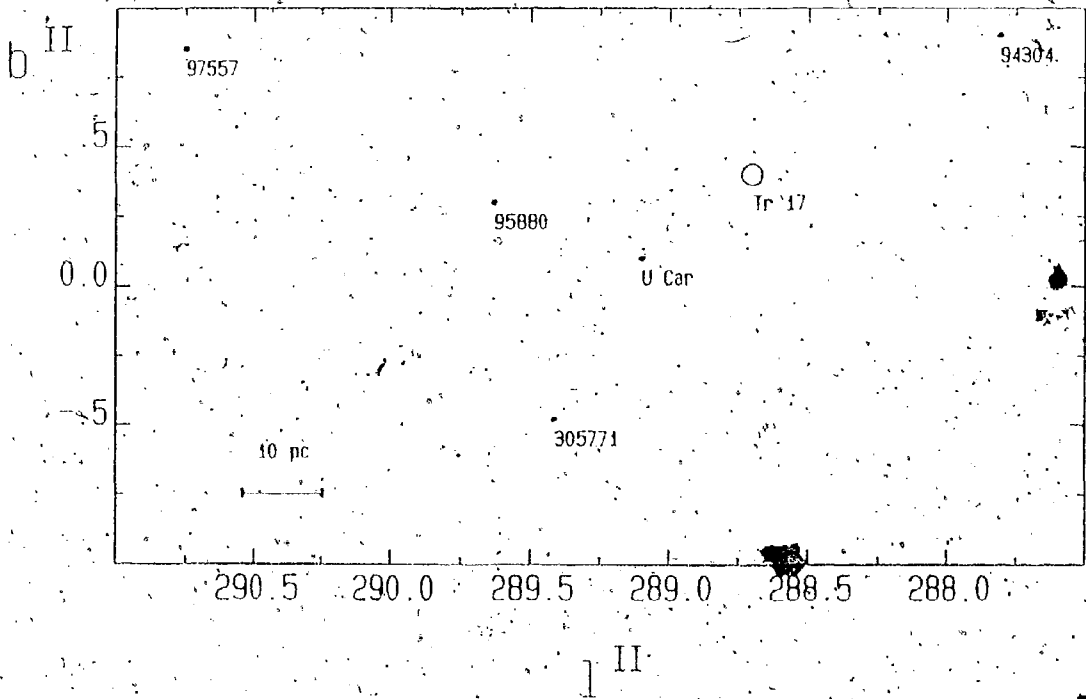
assuming a common origin for these objects. A velocity
dispersion of ±2.5 km/s agrees well with the expectations
for an association. A recent study by Mathieu (1983), for
example, reveals the velocity dispersion for the lambda
Orionis association to be ±2 km/s. We conclude that U Car
is quite likely associated with these 4 early-type stars,
having formed with them ~18My ago in a gravitationally
unbound cluster whose scattered members are still present
in the field. Furthermore, the data for these stars
indicate that they are older than and foreground to the
Car OB1 complex whose stars appear to be ubiquitous over
the field of this study. The derived luminosity for the
Cepheid U Car is <Mv>=-5.91, which is consistent with
existing P-L relations, given the star's long pulsational
period of 38.7614 days.

The plate material available for this thesis pre-
cluded the detection of any stellar group located at the
distance of the 13.2d Cepheid GT Car (~10.8 kpc).
Crowding of stellar images, especially on the B plate,
prevented an adequately complete sampling of the GT
Car field even at ~1.5 magnitudes brighter than would
have been required to detect a stellar group at the
distance of the Cepheid. Such a study must be deferred
until more suitable plate material or possibly CCD
imaging, preferably taken with a larger telescope, becomes

available.

Our analysis of the field of Trumpler 17 yielded a distance to the cluster of 2.0 ±0.4 kpc as compared to the 1.4 kpc suggested by Sher (1964). Sher's result was obtained by first estimating a mean reddening for the cluster from shifting the cluster sequence along a reddening line to best fit the ZAMS relation. This mean colour excess value was then used in a main-sequence fit to determine the distance modulus of the cluster. The result presented here, considering the obvious existence of differential reddening across the face of Trumpler 17, is likely more reliable. On the basis of distance and age considerations, we were able to reject the hypothesis that the Cepheid U Car originated in or is associated with this cluster.

We conclude that, in order to detect the presence of clusters or associations in the fields of long-period Cepheids, it is not sufficient to totally rely on the analysis of CC and CM diagrams. The need to detect a sufficient number of group members and the tendency of differential reddening to mask the existence of such stellar groups necessitates recourse to more sophisticated methods such as the variable extinction technique employed herein.

References

Baade, W., 1952, Transactions of the IAU, 8, 397

Baade, W., 1956, Publ. Astron. Soc. Pacific, 68, 5

Bohm-Vitense, E., 1981, Ann. Rev. Astron. Astrophys., 19, 295

Cloutman, L.D., and Whitaker, R.W., 1980, Astrophys. J.,
    237, 900

Dean, J.F., Warren, P.R., and Cousins, A.J.W., 1978, Mon.
    Not. R. Astron. Soc., 183, 569

Feast, M.W., 1958, Mon. Not. R. Astron. Soc., 118, 618

Fernie, J.D., 1963, Astron. J., 68, 780.

Fernie, J.D., and Hube, J.O., 1968, Astron. J., 76, 492

Fernie, J.D., 1969, Publ. Astron. Soc. Pacific, 81, 707

Flower, P.J., 1977, Astron. Astrophys., 54, 34

Garrison, R.F., 1970, Astron. J., 78, 1001

Garrison, R.F., Hiltner, W.A., and Schild, R.E., 1977,
    Astrophys. J. Suppl., 35, 111

Herbst, W., 1976, Ap. J., 208, 923

Hertzsprung, E., 1913, A.N., 196, 201

Humphreys, R.M., 1973, Astron. Astrophys. Suppl., 9, 85

Johnson, H.L., 1966, Ann. Rev. Astron. Astrophys., 4, 193

Kippenhahn, R., and Smith, L., 1969, Astron. Astrophys.,
    1, 142

Klare, G., and Neckel, Th., 1977, Astron. Astrophys.
    Suppl., 27, 215

Leavitt, H., 1912, Harvard College Observatory Circular 173, 1

Madore, B.F., 1975, Ap. J. Suppl., 29, 219

Maeder, A., 1981, Astron. Astrophys. 102, 401

Maeder, A., and Mermilliod, J.C., 1981, Astron. Astrophys.,
93, 136

Mathieu, R.D., 1983, Ap. J., 267, L97

Meyer-Hofmeister, E., 1972, Ages des Etoiles, IAU
Colloquim No. 17, p. XIX-1, eds. de Strobel, G.C.,
and Deplace, A.M., Observatoire de Paris: Meudon
France

Millward, C.G., and Walker, G.A.H., 1985, Astrophys. J.
Suppl 57, 63

Moffat, A.F.J., 1971, Astron. Astrophys., 13, 30

Moffat, A.F.J., 1972, Astron. Astrophys. Suppl., 7, 355

Moffat, A.F.J., 1974, Astron. Astrophys., 35, 315

Neckel, Th., and Klare, G., 1980, Astron. Astrophys. Suppl.,
42, 251

Pala, J., 1979, Honours Thesis University of Toronto unpub.

Parsons, S.B., 1971, Mon. Not. R. Astron. Soc., 15

Russell, H. N., 1913, Science, 37, 651

Schaefer, B.E., 1981, Publ. Astron. Soc. Pacific, 93, 253

Schaltenbrand, R., and Tammann, G.A., 1971, Astron. Astrophys.
Suppl., 4, 265

Schild, R. E., Garrison, R.F., and Hiltner, W.A., 1983,
Astrophys. J. Suppl., 51, 321

Shapley, H., 1918, Ap. J., 48, 89

Sher, D., 1964, Mon. Not. R. Astron. Soc., 129, 237

Steppe, H., 1977, Astron. Astrophys. Suppl., 27, 415

Stibbs, D.W.N., 1955, Mon. Not. R. Astron. Soc., 115, 363

Tammann, G.A., 1970, IAU Coll. 37, 236

Trumpler, R.J., 1930, Lick Observatory Bull. 14, # 420, 5,

Turner, D.G., 1976, Astron. J., 81, 97

Turner, D.G., 1980, Astrophys. J., 240, 137

Turner, D.G., Grieve, G.R., Herbst, W., and Harris, W.E.,
    1980, Astron. J., 85, 1193

Turner, D.G., Leonard, P.J.T., and English, D.A., 1987,
    Astron, J., 93, 368.

Turner, D.G., and Moffat, A.F.J., 1980, Mon. Not. R. Astron.
    Soc., 192, 283

van den Bergh, S., and Harris G.L.H., 1976, Ap. J., 208, 765

van den Bergh, S., 1977, Decalages vers le Rouge et Expan-
    sion de l'Univers, IAU Colloquium No. 37, Eds. Balkow-
    ski, C., and Westerlund, B.E., (Paris, C.N.R.S.), p13

van den Bergh, S., 1985, in IAU Coll. 82, Cepheids: Theory
    and Observations, Madore, B.F., ed., Cambridge Univer-
    sity Press, Cambridge, 1985

van den Bergh, S., Brosterhus, E.B.F., and Alcaino, G.,
    1982, Ap. J. Suppl., 50, 529.

van den Bergh, S., Brosterhus, E.B.F., and Alcaino, G.,
    1983, Ap. J. Suppl., 53, 765

van den Bergh, S., Younger, P.F., and Turner, D.G., 1984,

    Ap. J. Suppl., <u>57</u>, 743

Curriculum Vitae

Name: Terence A. Danks

Date and Place of Birth: March 5, 1944   Toronto, Ontario

Post-Secondary Education:

   Concordia University (Loyola of Montreal)
   1961-1965   B.Sc.   Physics

   Department of Transport
   Air Services Training School
   Ottawa, Ontario
   Introduction To Meteorology

   (Observing Procedures and Codes)
   June - July 1966

   Department of Transport
   Meteorological Branch Headquarters
   Toronto, Ontario
   Theoretical and Applied Meteorology

   (Meteorological Officer Course No. 23)
   July - Dec 1966

   Canadian Forces School of Meteorology
   Canadian Forces Base Trenton
   Meteorological Operations

   Jan - Mar 1967

   Maritime Command Warfare School
   Canadian Forces Base Stadacona
   Maritime Warfare and Military Oceanography

   February 1976

Royal Roads Military College
Victoria, B.C.
Introduction to Physical Oceanography
-------------- -- --------- -------------

June 1983

Employment History:

Research Assistant
Concordia University (Loyola of Montreal)
Department of Physics
June 1965 - May 1966

Meteorological Officer
Yukon Weather Office
Whitehorse, Y.T.
1967 - 1975

Duty Meteorologist
Maritimes Weather Office
Bedford, N.S.
1976

Duty Meteorologist
Canadian Forces Meteorological and
Oceanographic Centre
Maritime Command Headquarters, Halifax, N.S.
1976 - 1982

Supervising Meteorologist
Canadian Forces Meteorological and
Oceanographic Centre
Maritime Command Headquarters, Halifax, N.S.
1982 -